Origin of scatter in paleomagnetic directions of samples from Gorely Volcano, Kamchatka, Russia

This senior thesis
is submitted to
the faculty of
Western Washington University

To fulfill part of the requirement for
graduation with honors from the
Department of Geology

by

Colleen Riley

June 9, 1994

Origin of scatter in paleomagnetic directions of samples from Gorely Volcano, Kamchatka, Russia

by

Colleen Riley

Accepted in partial completion
of the requirements for
graduation with honors from the
Department of Geology

Approved by

Russell F. Burmester, Ph.D.

Abstract

Lava flows from sixteen sites at Gorely Volcano, Kamchatka were sampled. Initial analysis showed high within-site scatter for NRM specimen directions. Alternating field and thermal demagnetization of specimens showed single-component magnetization indicating that specimens had not moved or were not exposed to changes in the magnetic field during acquisition of a magnetic direction. Scatter is thought to be either due to movement of the specimen with respect to the magnetic field or change in the magnetic field with respect to the specimen. Four factors were found that would contribute to scatter in specimen directions. These are 1) cooling rate, 2) range of unblocking temperatures, 3) relative time of emplacement, and 4) how the specimen moved or was affected by changes in the magnetic field. Only two sites showed that scatter was due to movement of the specimen. It appears that scatter in other sites resulted from changes in the magnetic field generated from a magma-induced electrical current due to lava flowing in the earth's magnetic field. These changes in the magnetic field are shown to have more affect on material sampled at the surface than on material sampled at depth because massive interiors of flows showed less dispersion in specimen directions than levees or pull-aparts.

Introduction

The ability to predict volcanic eruptions is an important part of hazards assessment in volcanic areas. In order to predict an eruption, it is helpful to know the eruptive history of a volcano so that its eruptive cycle can be determined. Once an eruptive cycle is determined, the volcano's current activity, morphology, or magma chemistry can be placed within it's eruptive cycle. This makes it possible to predict when an eruption might occur, what magnitude that eruption might be, and what areas might be in danger, so that measures can be taken to prevent loss of life (Wright and Pierson, 1992).

The eruptive cycle for Kilauea volcano in Hawaii has been determined, and is based on several eruptive cycle models. This volcano has been studied extensively and its deposits dated by various methods including Carbon-14 (Lockwood and Lipman, 1980) and paleomagnetic secular variation (Holcomb et al., 1986). The dating of volcanic deposits allows eruptive-cycle models to be developed. One such model, based on caldera collapse, shows a cycle beginning with sustained summit eruptions that become intermittant and infrequent with time (Fig. 1). Other eruptive-cycle models for Kilauea have been developed based on flank eruptions and the combination of flank eruptions and caldera collapse patterns. All of these eruptive-cycle models are based on patterns shown in

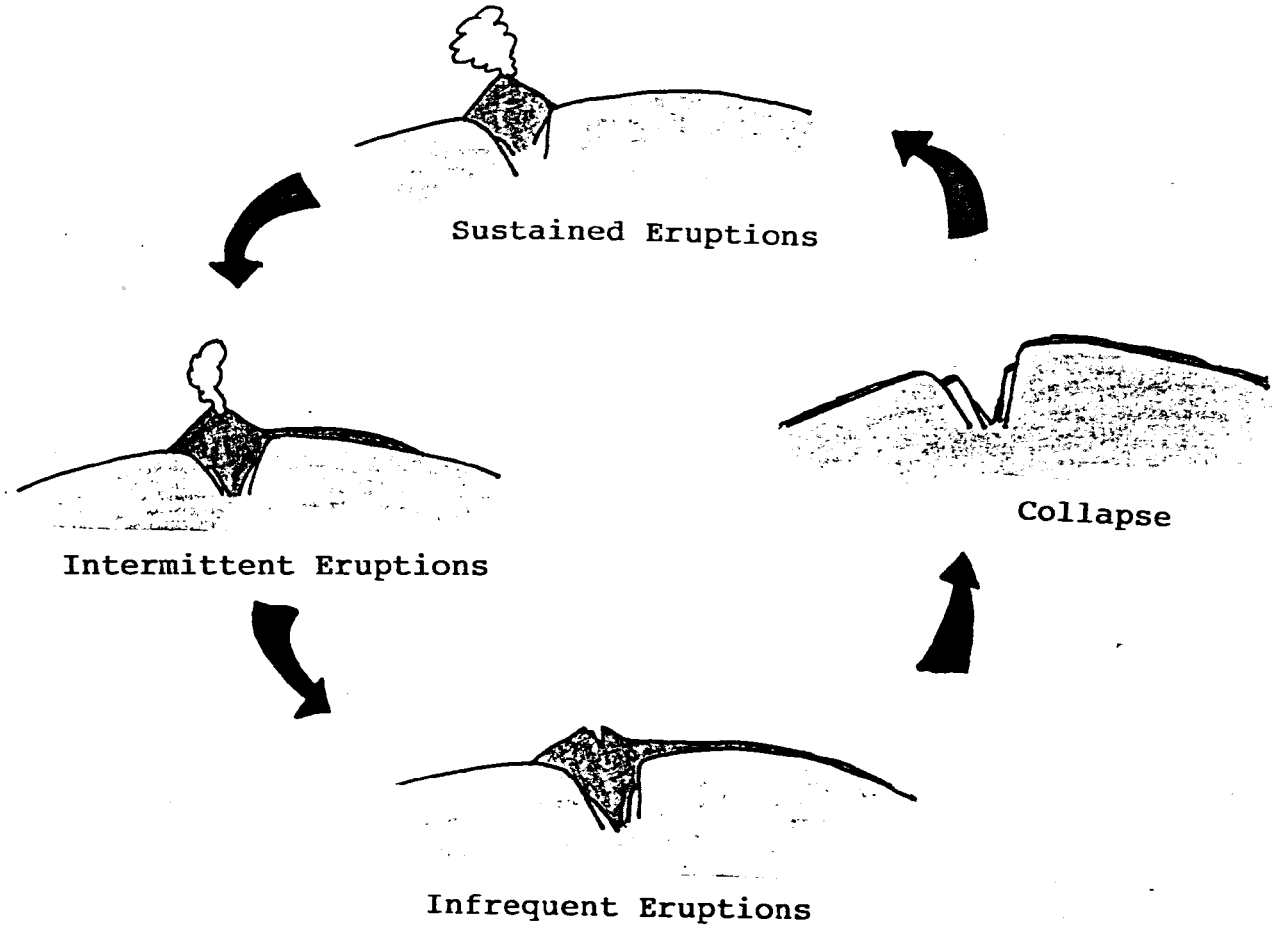

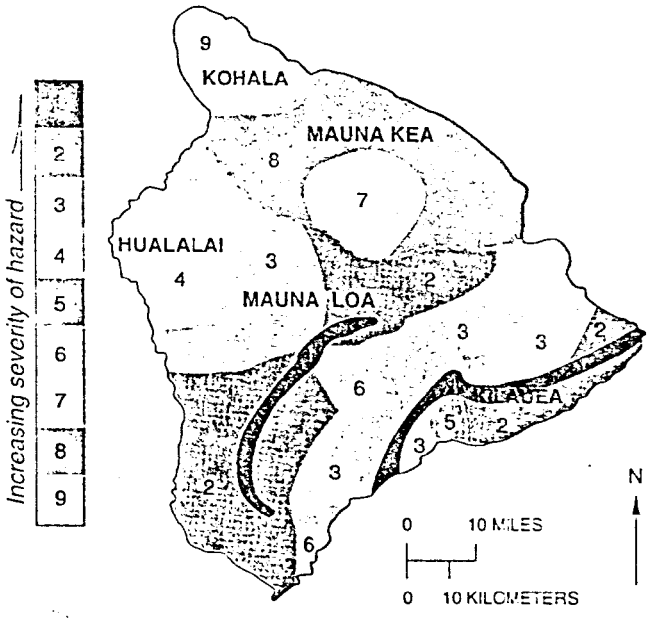

Fig. 1 Cyclic Model for summit eruptions at Kilauea based on caldera collapse. This model and others like it are based on information from volcanic deposits. (Simplified from Holcomb, 1987)

Fig. 2 Map showing hazard zones for the island of Hawaii. These zones are determined using data from volcanic deposits. (from Wright and Pierson, 1992)

dated volcanic deposits. This allows future eruptions to be predicted and the degree to which hazards might effect different areas to be determined (Holcomb, 1987). Fig. 2 shows a hazards map of the island of Hawaii.

The oceanic island volcanism of Kilauea is not as violent as volcanism found in continental magmatic arcs such as the Cascade Arc or Kamchatka Arc. The determination of eruptive cycles for volcanoes in these arcs are potentially of far more importance because of their more violent eruptive potential. However, such arc volcanoes are not as well studied as oceanic island volcanoes.

The violent nature of magmatic arc volcanism was displayed on May 18, 1980, when Mount St. Helens erupted. Such an eruption was predicted by Crandell and Mullineaux (1978) who had studied the volcano's deposits. They were able to determine eruptive cycles for the past 4,500 years that indicated periods of dormancy lasting 100-200 years and 600-700 years. They placed the current activity of the volcano within it's eruptive cycle and forecast a violent eruption, "...perhaps even before the end of this century" (Decker, 1981).

The eruption of Mount St. Helens demonstrates the importance of determining the eruptive cycles for volcanoes. To do this, the deposits from eruptive events of a volcano must be dated. Dating these deposits allows us to determine the relative size, nature, and frequency of past eruptions. Using this information, hazard maps can be produced (Fig. 3)(Wright and Pierson, 1991).

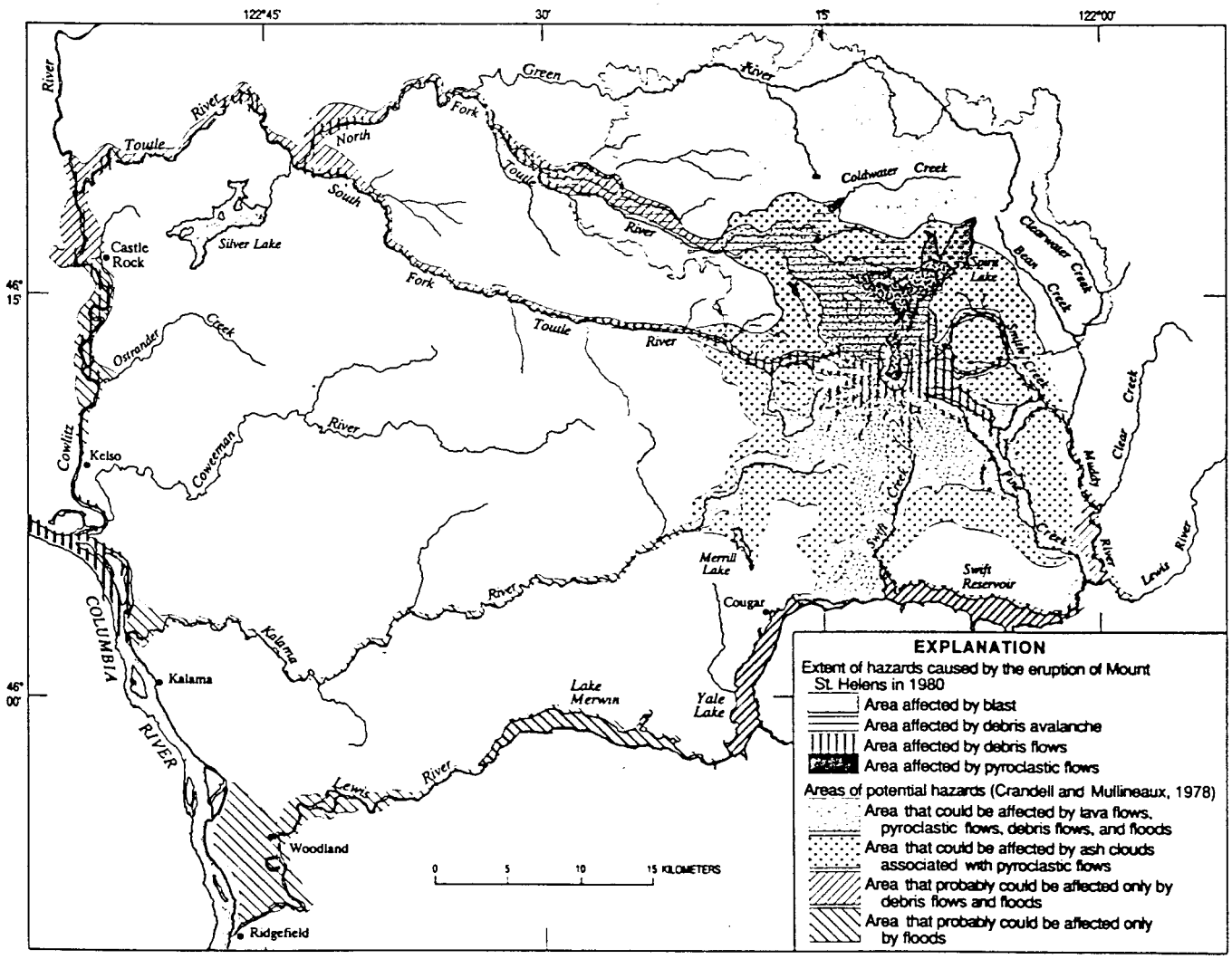

Fig. 3 Hazards map for Mount St. Helens showing areas of potential hazards as outlined by Crandell and Mullineax (1978) and areas effected by the 1980 eruption (from Wright and Pierson, 1992).

Determining absolute dates for eruptive events allows the behavior of a volcano and its magmatic changes through time to be established. If eruptive cycles for several volcanoes in an arc are determined from these events, volcanic eruptions can be compared from different areas and possible patterns of synchronicity established. Perhaps with better dating methods, present theories concerned with apparent patterns of synchronicity can be tested (Scott, 1990). Dating volcanic events would also allow us to determine possible relationships to tectonic state or changes that might influence eruptive cycles, such as dip angle of the subducting plate, rate of subduction, tectonic stress and slip events (Zharinov and Demin, 1989), and migration of magma along faults (Leonov, 1990).

Background

Both the Cascade and Kamchatka Arcs (Fig. 4) contain volcanoes that have violent eruptive potential, as exemplified by the eruption of Mount St. Helens and the more recent eruption of Bezymianny (Mockler, 1993). Volcanoes in both arcs are very similar in eruption type, magnitude, and deposits (see Bogoyavlenskaya, 1985). Because of this similarity, research conducted in either region would benefit both regions.

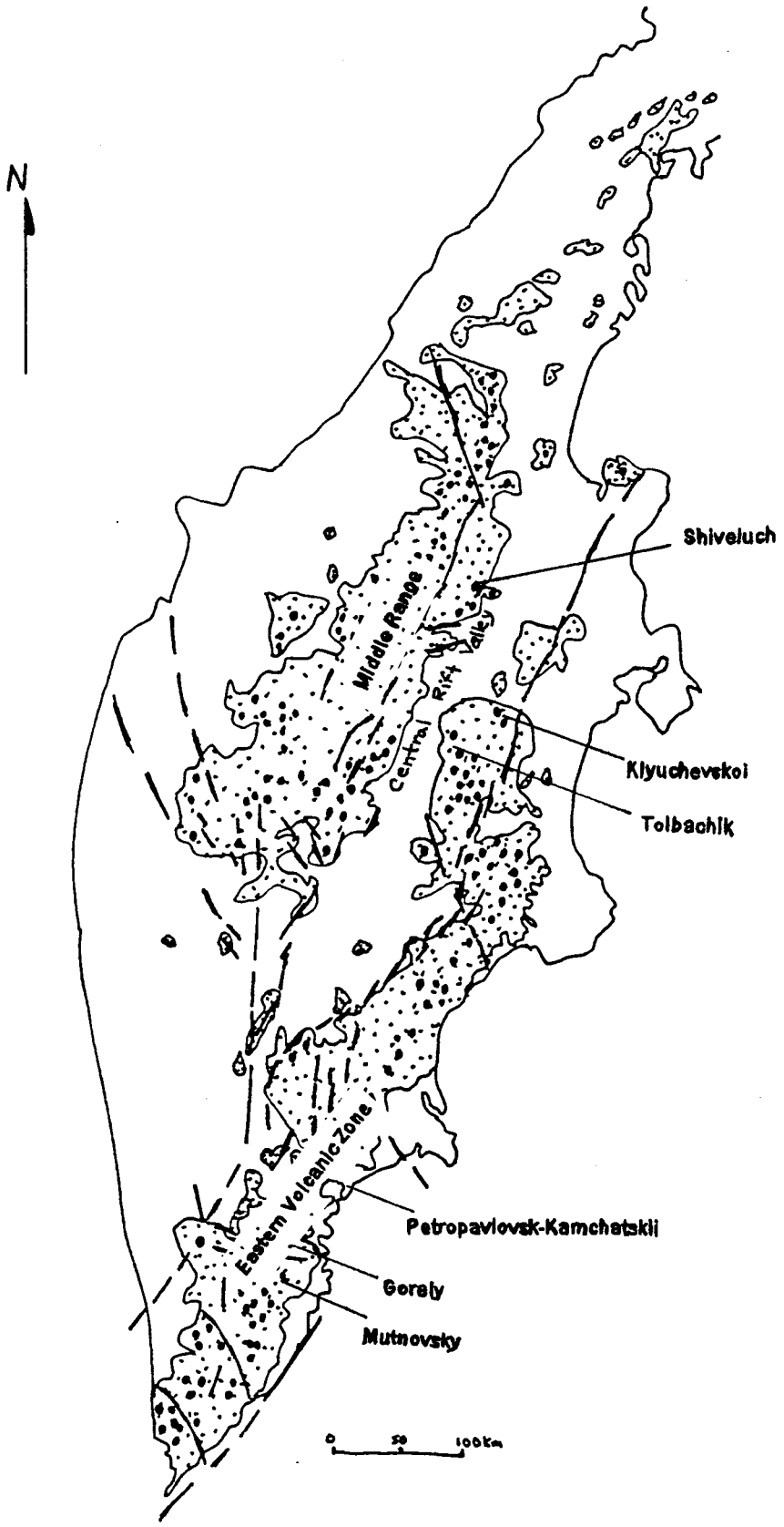

Fig. 4 Map of Kamchatka showing the distribution of volcanic deposits (stippled pattern), faults, and volcanoes (represented by filled circles). Gorely is located in southeast Kamchatka in the Eastern volcanic zone. (compiled from Florenskii and Trifonov, 1985 and Leonov, 1991)

Data on eruptive cycles for the Cascade Arc show that a third of the events or groups of events are not dated (Fig. 5; Scott, 1990). The time span studied was 15,000 years. A quarter of this time appears to be hiatuses in activity. Some of these apparent hiatuses can be attributed to an incomplete record of eruptions for volcanoes whose deposits could not be dated by Carbon-14 or by other methods such as dendrochronology. If the record were to include data from these undated events, periods of inactivity might be diminished and a more complete record for eruptive cycles determined (Scott, 1990).

Tephrachronology in conjunction with Carbon-14 has been used to date volcanic deposits in the Tolbachik Valley, Kamchatka. The results have been used to date layers of tephra exposed in pits . Each of these pits reveals a stratigraphic column for the site (Fig. 6). Unfortunately, not all sites containing valuable information about eruptive cycles have suitable amounts of tephra (Braitseva et al., 1983). Clearly another method is needed to date events in Kamchatka that have sparse amounts of tephra and events in the Cascade Arc that can not be dated by Carbon-14 or dendrochronology.

Methods used to date eruptive events

Many methods have been used to date eruption deposits. Which method is used depends upon the kind of deposit

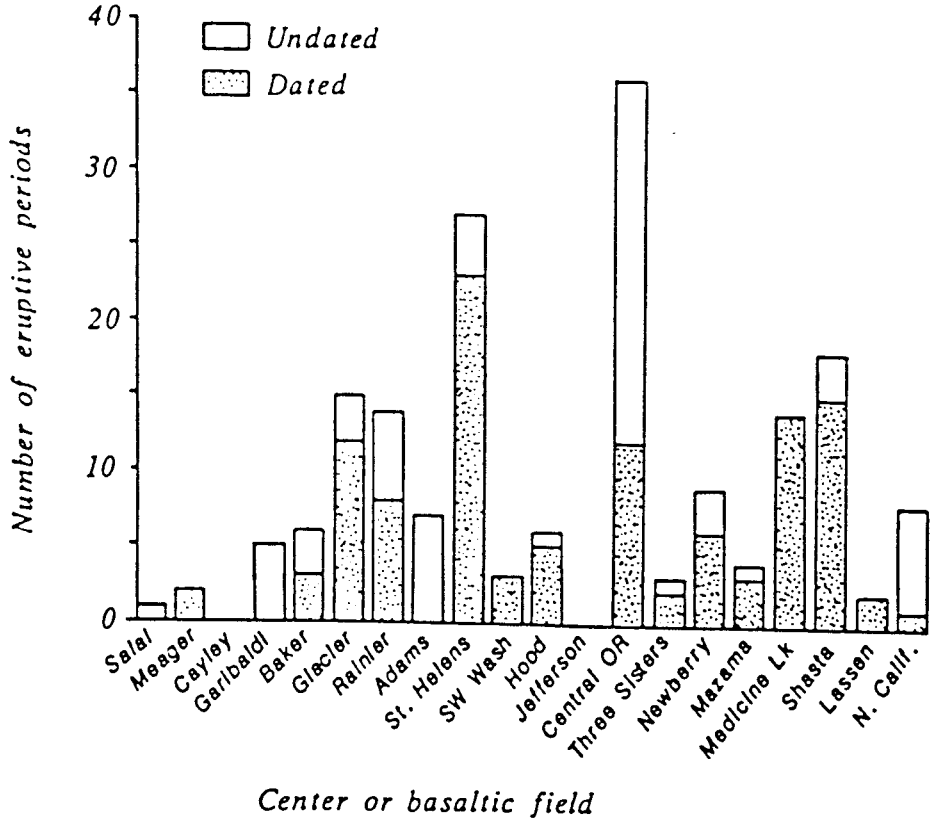

Fig. 5 Graph showing number of undated and dated eruptive periods for Cascade Arc volcanoes. If undated eruptive periods can be dated, apparent hiatuses in activity might be diminished (from Scott, 1990).

Fig. 6 Pit at Gorely Volcano showing ash layers that were used for correlation in tephrachronology.

left by the eruption. A less explosive eruption, such as the kind in Hawaii, would produce basaltic lava flows that have little or no tephra associated with them. Or, as in the case of Kilauea, the associated tephra is deep beneath younger lava flows (Holcomb et al.,1986). These flows could be dated by carbon-14 from charcoal beneath them, by multispectral thermal infrared imaging, or by paleomagnetic secular variation. A more explosive eruption, such as those in the Cascade Arc or Kamchatka Arc, might produce lava and tephra or only tephra. The tephra could be dated by tephrachronology or thermoluminesence.

Tephrachronology is a relative dating method that uses tephra layers to compare sites. Stratigraphic columns from each site are compared and tephra layers from widespread ash fall are matched from one site to another on the basis of texture, color, and mineral content. Sites may contain different thicknesses of ash depending on distance from the volcano and wind direction. The stratigraphic columns from different sites may be correlated using tephra from eruptions of neighboring volcanoes or tephra layers may be absent (see Fig. 7 for an example of how this method is used). Once layers are matched between sites , layers that may be missing at different sites help create a more complete stratigraphic column. Relative ages of eruptions that created these tephra layers then can be determined over wide areas. Carbon-14 dates (given by dating charcoal within the tephra), provide

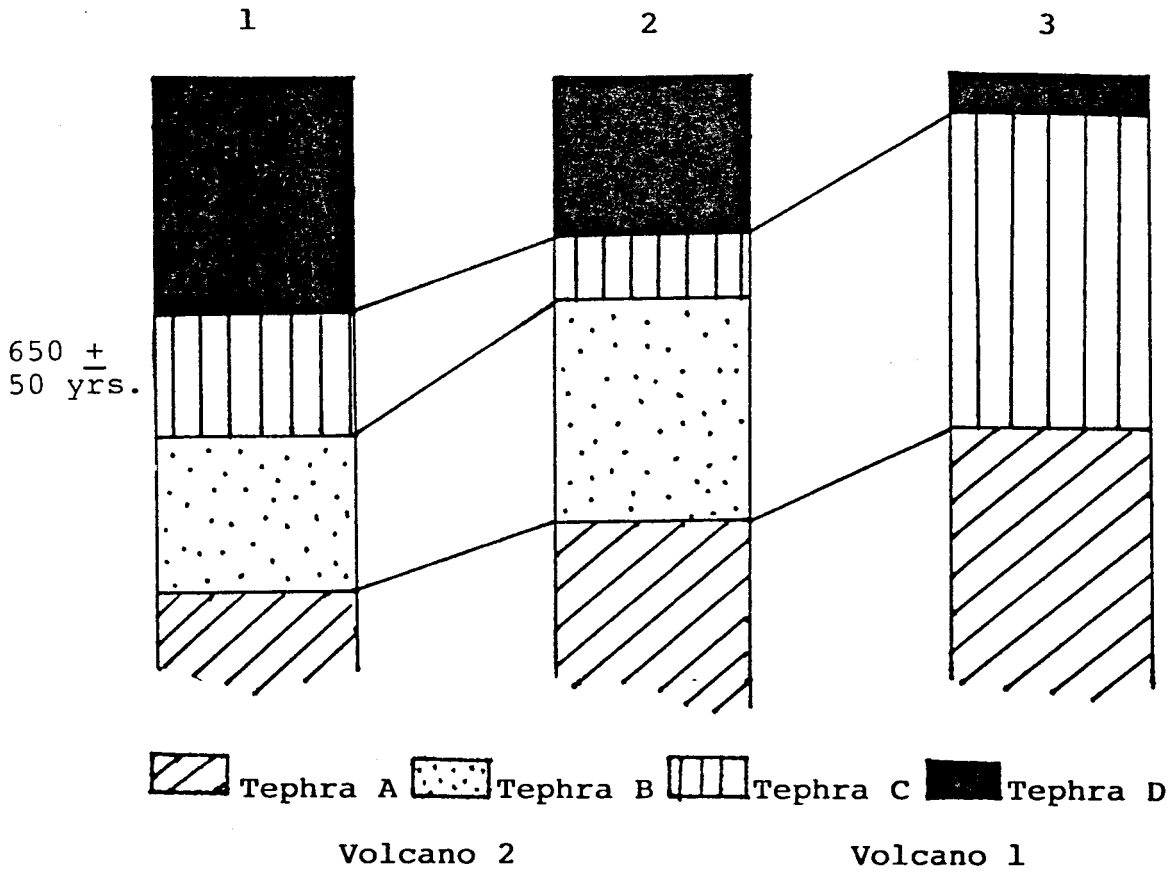

Fig. 7 Correlation of Stratigraphic Columns by Tephrachronology. Column 1 is located closest to volcano 1 and column 3 is located closest to volcano 2. Column 3 is missing a tephra layer and so gives an incomplete record of eruptions for volcano 1. By comparing this column to other columns, such as column 1, and correlating tephra layers D and B of column 1 with D and B of column 3, tephra layer C is found to be missing. Tephra is missing in column 3 because ash did not reach this distance. A date given by charcoal in column 1 for tephra C can be used to date the correlated tephra in column 2.

absolute dates that can be assigned to tephra layers. However, tephra is not associated with some sites that might give a more detailed record of past eruptions because of conditions that are not favorable to deposition or preservation, such as wind direction, distance from volcano, or eruption type (Braitseva et al., 1983).

Thermoluminesence dating has been used to date volcanic glass, and has been used successfully to give absolute dates to tephra 100 to 400,000 years old. Application of this method is limited by the size of the glass shards, which must be between 4 and 11μm, and by the composition of the glass shards, which should not contain imbedded minerals. Thermoluminesence uses the amount of energy built up in electron traps to determine the age of a sample. Electron traps are zeroed at the last heating, so volcanic glass shards must be carefully selected to represent original heating at the time of deposition (Berger, 1991). A lava flow must be associated with tephra in order to be dated by thermoluminesence, so as with tephrachronology, areas that do not have tephra or have sparse amounts of tephra cannot be dated by this method.

Multispectral thermal infrared imaging has also been used to date lava flows. It is a relatively new method that is based on the weathering of a lava's crust, iron-oxide content, and state of devitrification. This method gives relative dates to lava flows based on the color gotten from multispectral thermal infrared imaging.

The method requires that areas be sparsely vegetated. Because weathering rates differ from place to place, color from imaging will be dependent upon the environment (Kahle et al., 1988).

Carbon-14 dating of charcoal under lava flows from Hawaii has been used by Lockwood and Lipman (1980) to date the lava flows. This requires conditions in which the flow overrode vegetation and was hot enough to carbonize wood but not so hot that the wood was burnt and consumed.

Paleomagnetic secular variation has also been used to date lava flows. To do this, paleomagnetic directions are obtained from rocks at different sites that have been dated by Carbon-14 or other methods. These directions are then plotted and a curve is fit to the points in order of age, which indicates how the magnetic field changed through time. This curve then becomes the paleomagnetic secular variation reference curve for the area. Directions from samples that cannot be dated by other methods can be compared with this secular variation curve. The age of the sample is given by the part of the curve that comes closest to the samples' direction. Figure 8 gives two examples of secular variation curves from Hawaiian lava flows (Holcomb et al., 1986).

Holcomb et al. (1986) used secular variation curves to date lava flows in Hawaii. They found that aa flows gave more dispersion than did pahoehoe flows and that lava channels and tubes also had high dispersion. They suggest that the interior of pahoehoe flows have the

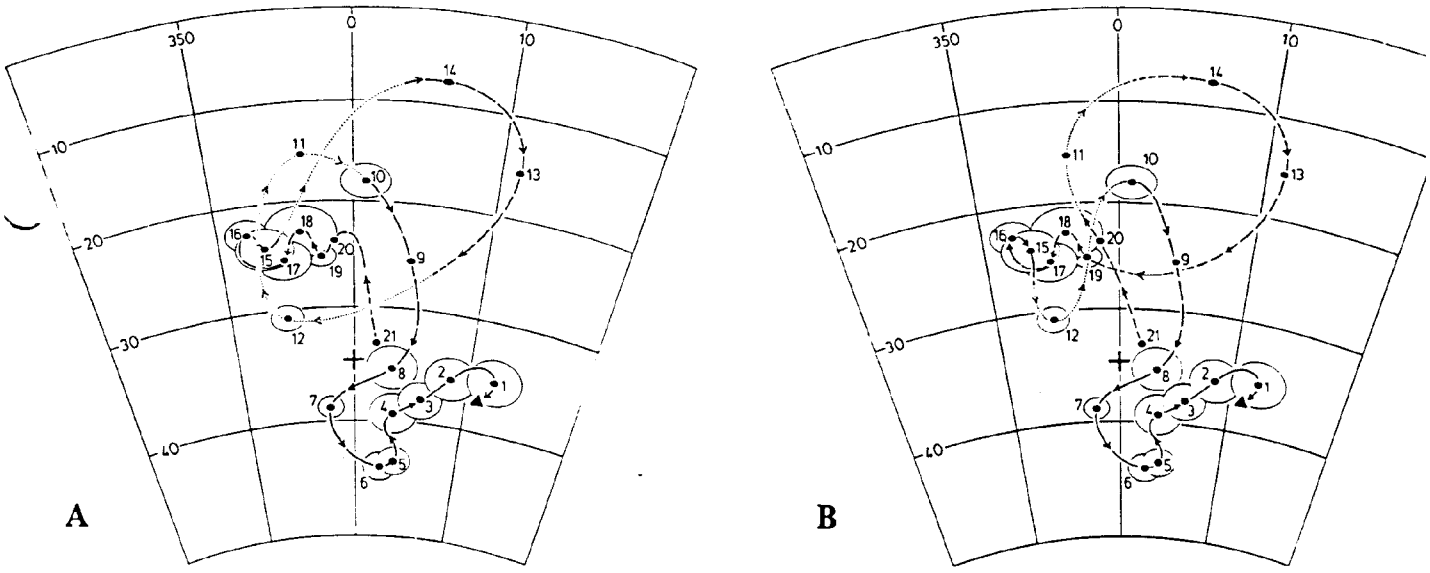

Fig. 8 Secular variation curves of Hawaii. Secular variation curves can be used to date lava flows. The curves are based on directions from flows that were dated by other methods. Curves A and B show secular variation for the last 3000 years. These curves are different because of uncertainty in the age of 12.

lowest dispersion because they cool faster and have less chance of being moved after cooling.

Holcomb et al. (1986) observed several problems in using the secular variation curve method. One problem is that curves covering older time spans were less reliable than curves covering younger time spans. The reason for this is that curves covering older dates were based on fewer samples that had less reliable dates. They also found that the secular variation curves yielded ambiguous dates in areas where the curve crossed itself. Another problem with secular variation curves is that they are not universally applicable. This is because secular variation history varies from locality to locality. Also, some rocks may not be suitable for use with this method because their magnetization may be too low or unreliable (Holcomb, 1986).

There are several advantages to the secular variation curve method. The use of secular variation curves gives a method for dating lava flows that is not dependent on climate or environment, as is multispectral thermal infrared imaging, and can give absolute dates for areas not associated with tephra or vegetation (Holcomb, 1986).

Previous Work

Dating lava flows with secular variation curves in areas not associated with tephra or vegetation is useful. Kamchatka is a good area to use secular variation

dating because previous tephra research can serve as a control. Volcanism in Kamchatka is similar to Cascade Arc volcanism and so research done there would benefit both areas.

Research done on tephra in Kamchatka produced a tephra stratigraphic column calibrated with Carbon-14 dates (see Fig. 9). These dates are somewhat contraversial because seperate studies gave different Carbon-14 dates for marker beds of tephra from Shiveluch Volcano (Braytseva et al., 1983). The dates from this study were used by Kochegura ~~Zubov (unpublished)~~ to calibrate a secular variation curve for tephra in Kamchatka ~~the Tolbachik Valley~~. Some work also was done around Mutnovsky Volcano, which is near Gorely Volcano (Fig. 10). This research makes Gorely Volcano an excellent test area for the use of secular variation curves to date volcanic deposits.

Gorely volcano is located south of the Tolbachik Valley in the Eastern Volcanic Zone. Mutnovsky Volcano neighbors it to the southeast (see Fig. 4 and 11). Gorely Volcano has lava flows that are not associated with tephra which makes these flows good candidates for secular variation dating. A stratigraphic column from Mutnovsky Volcano can be used to correlate tephra from Gorely (Fig. 12) and the secular variation curve by Zubov can be used to date the lava flows. The dates from the secular variation curve can then be used to compare those gotten from correlating the tephra.

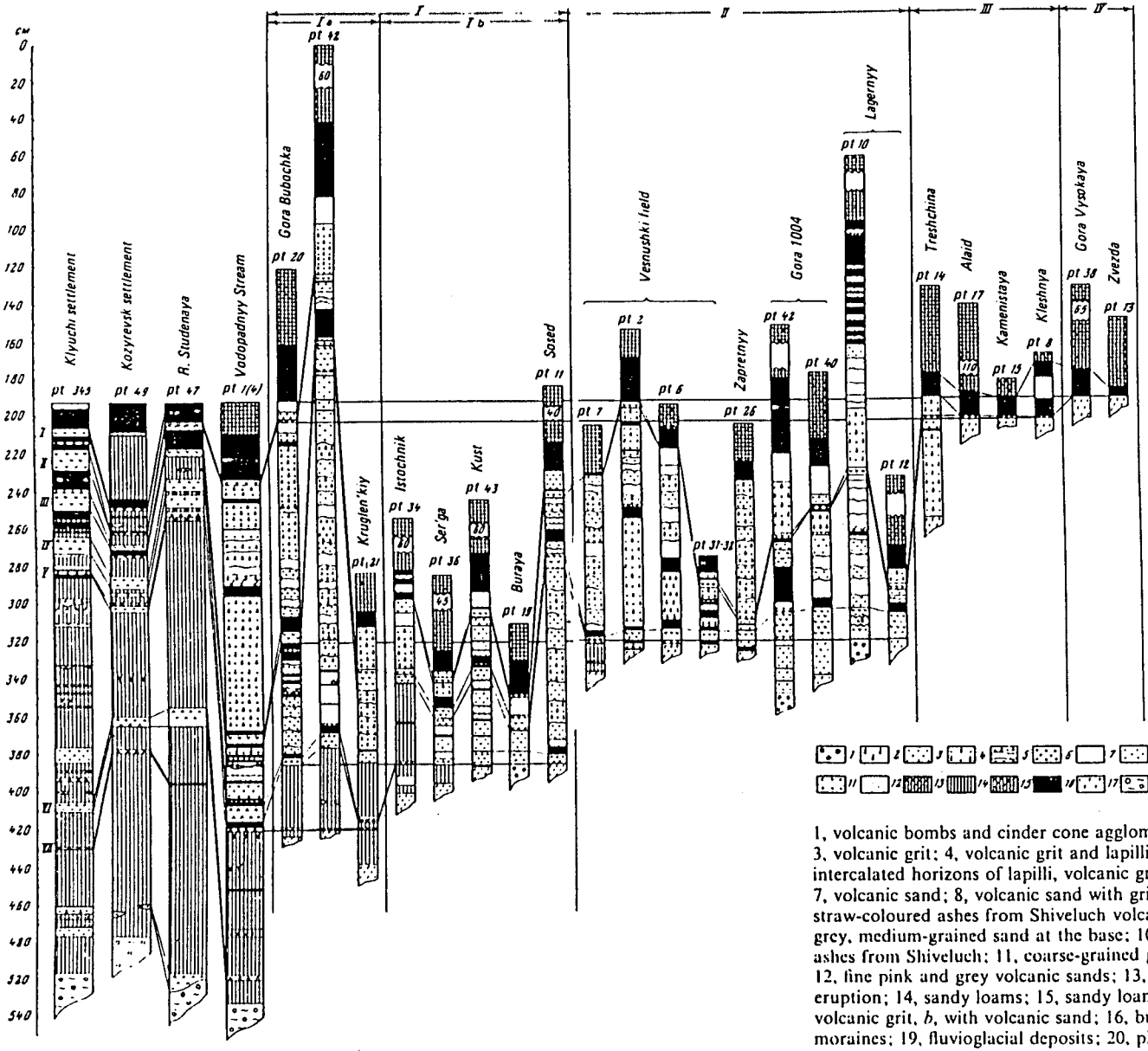

1, volcanic bombs and cinder cone agglomerates; 2, scoriaceous lapilli; 3, volcanic grit; 4, volcanic grit and lapilli; 5, stratified tephra: intercalated horizons of lapilli, volcanic grit and sand; 6, pumice grit; 7, volcanic sand; 8, volcanic sand with grit; 9, fine white and straw-coloured ashes from Shiveluch volcano: *a*, uniform, *b*, with grey, medium-grained sand at the base; 10, fine yellow and cream ashes from Shiveluch; 11, coarse-grained grey-yellow volcanic sand; 12, fine pink and grey volcanic sands; 13, tephra from the 1975–76 eruption; 14, sandy loams; 15, sandy loams, saturated: *a*, with volcanic grit, *b*, with volcanic sand; 16, buried soils; 17, basalts; 18, moraines; 19, fluvioglacial deposits; 20, plant remains. I-VIII, main marker horizons of Klyuchi ash.

Fig. 9 Stratigraphic columns showing correlation of tephra in the Tolbachik Valley, Kamchatka (Braytseva et al., 1983).

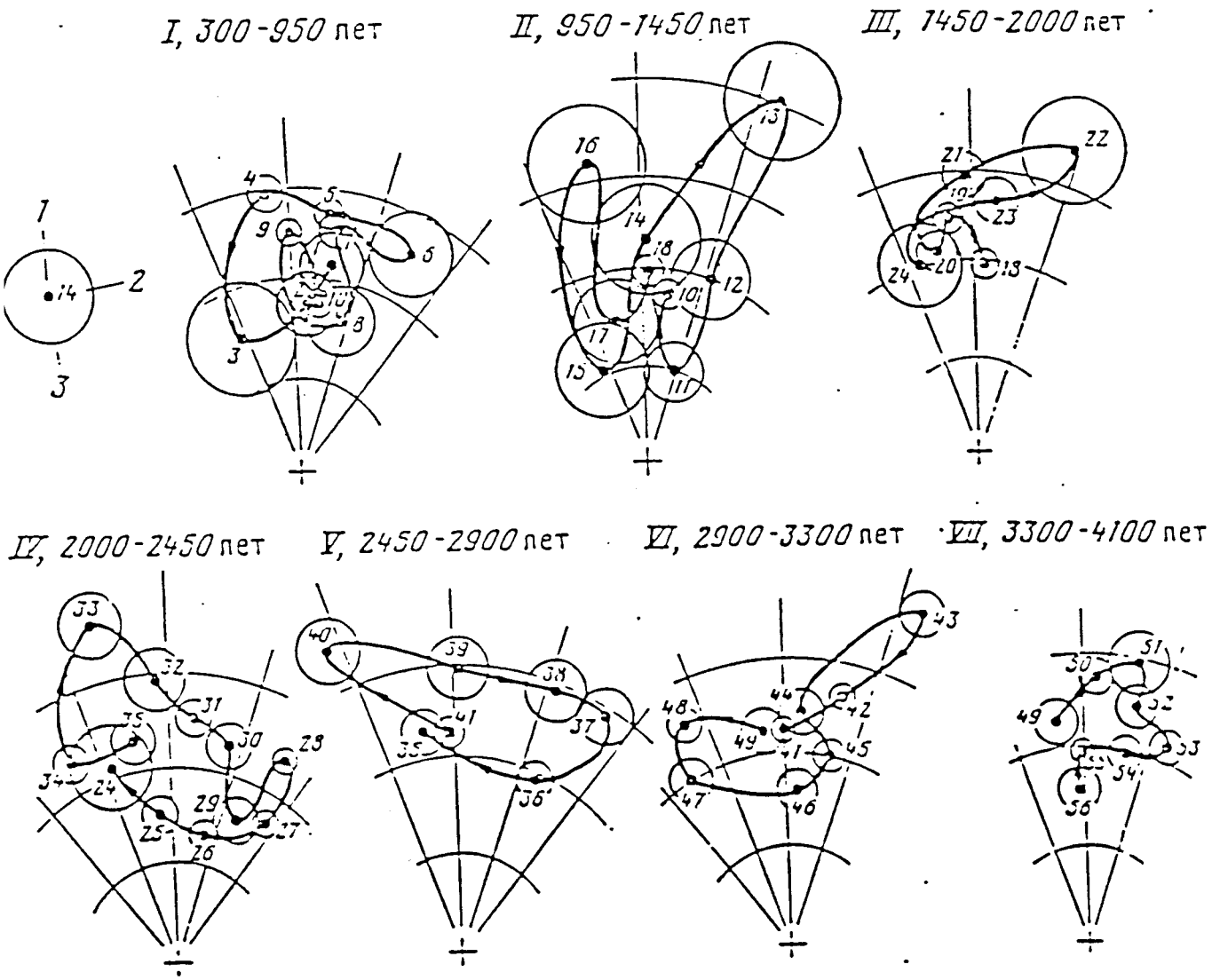

Fig. 10 Secular variation curve for dated tephra from ~~the Tolbachik Valley,~~ Kamchatka ~~(Zubov, unpublished)~~. I through VII separate the curve into short age ranges, net = year. (Kochegura et al., 1990)

Fig. 11 Map showing the location of Gorely and Mutnovsky Volcanoes. Dark arrow indicates their location.

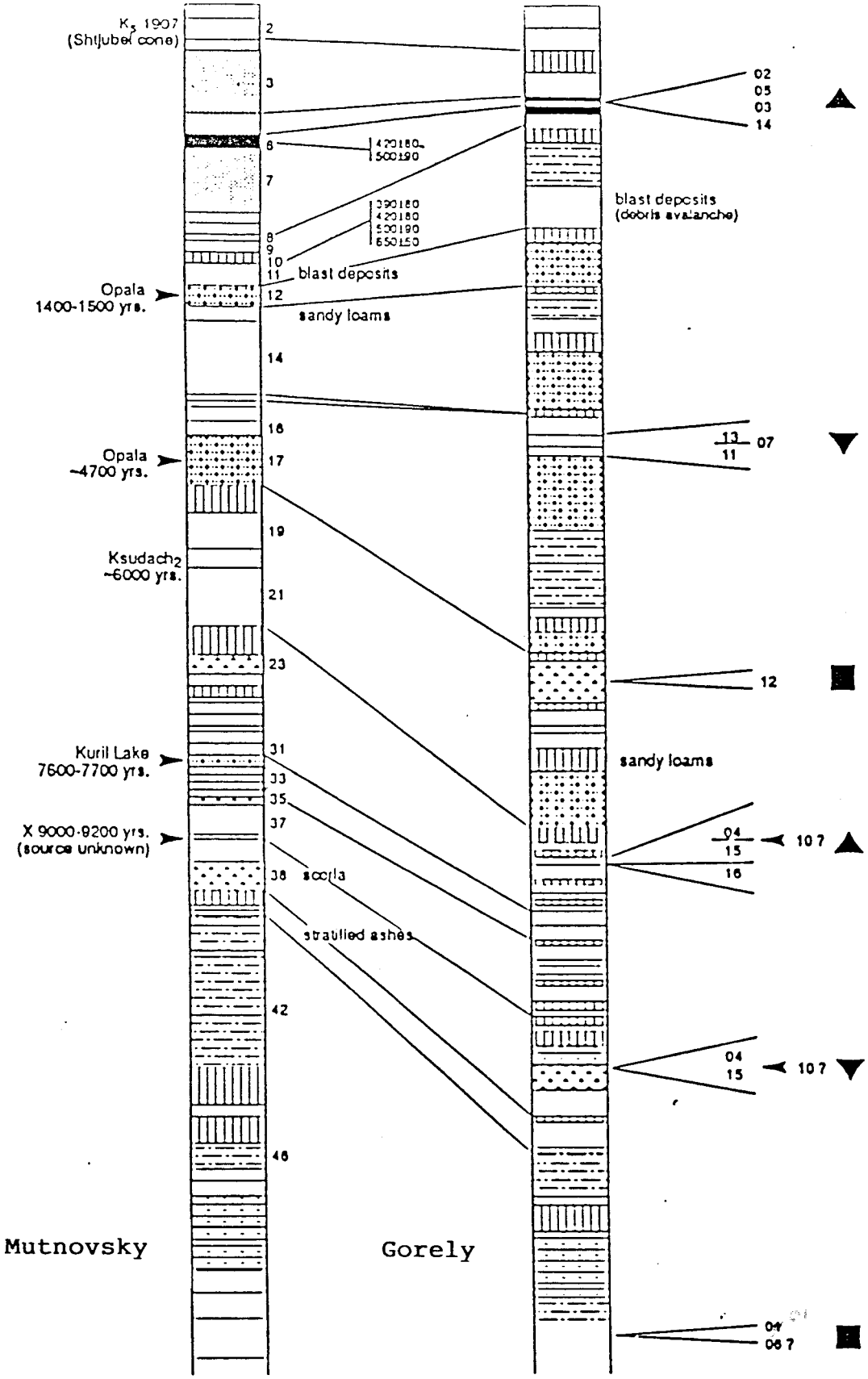

Fig. 12 Stratigraphic columns from Mutnovsky and Gorely Volcanoes. Numbers for the Mutnovsky column indicate horizons sampled by Zubov (unpublished). Sites in this study are grouped by age, with the age determined by correlating tephra layers from Gorely with those from Mutnovsky (Ponomareva, unpublished). Symbols in the right most column are used in Figs. 12 and 14.

Burmester (unpublished) used Zubov's secular variation curve to test secular variation dating of lava flows using Hawaiian -style sampling methods (Fig. 13). The NRM results obtained by Burmester were much more scattered than typical in Hawaii (Fig. 14), and some sites did not fit Zubov's secular variation curve, raising questions about why the methods that proved so useful in Hawaii seemed to fail. The purpose of this study is to determine why the directions obtained by Burmester for samples from Gorely Volcano had high within-site scatter.

Methods

Sixteen sites were sampled around Gorely Volcano. Site locations are shown in Figure 15. All sites sampled, except one, were from flows of basaltic andesite. The exception was an aglutinated cinder cone. Samples show a wide range of textures from vesicular to porphyritic.

Sites were selected to avoid lava that had been transported or tilted after cooling. Most samples were taken from levees under the assumption that lava there would cool faster and be less likely to have been transported than lava in the middle of the flows or channels. Pull aparts were also sampled under the same assumption (Fig. 16).

Sites were sampled using a gasoline-powered drill equipped with a 2.5 cm diameter, nonmagnetic drill bit. Samples were oriented *in situ* by magnetic and sun compass.

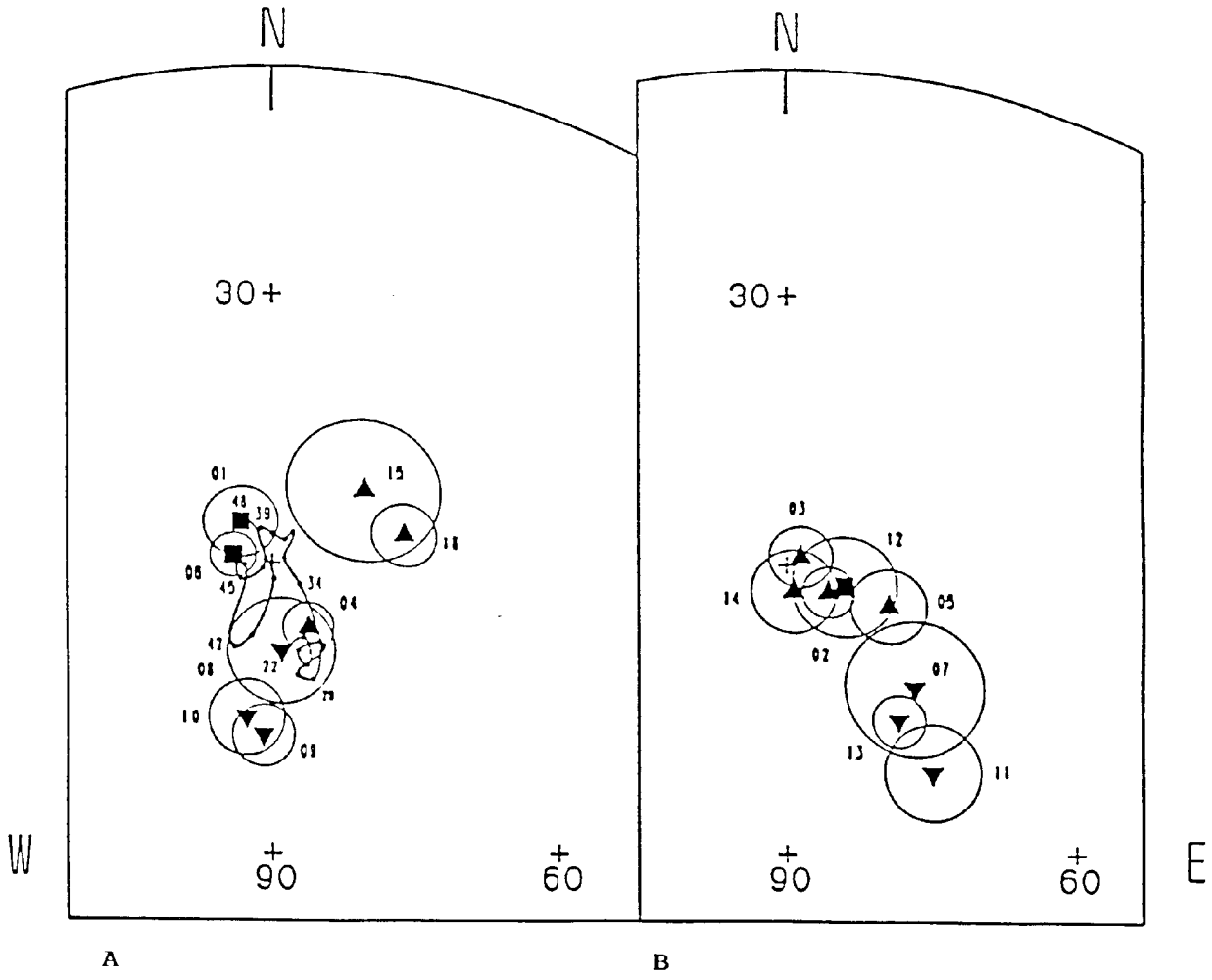

Fig. 13 Equal-area plots showing site mean directions for sites at Gorely Volcano and their alpha-95 cones of confidence. A) shows directions for older flows compared to a secular variation curve from neighboring Mutnovsky Volcano (Zubov, unpublished). The smaller numbers refer to Zubov's horizons (left column, Fig. 11); the larger numbers are sites at Gorely (right column, Figs. 11 and 14). B) shows directions for flows younger than the secular variation curve. Symbols denote flows expected to have the same direction based on tephra correlation (Fig. 11).

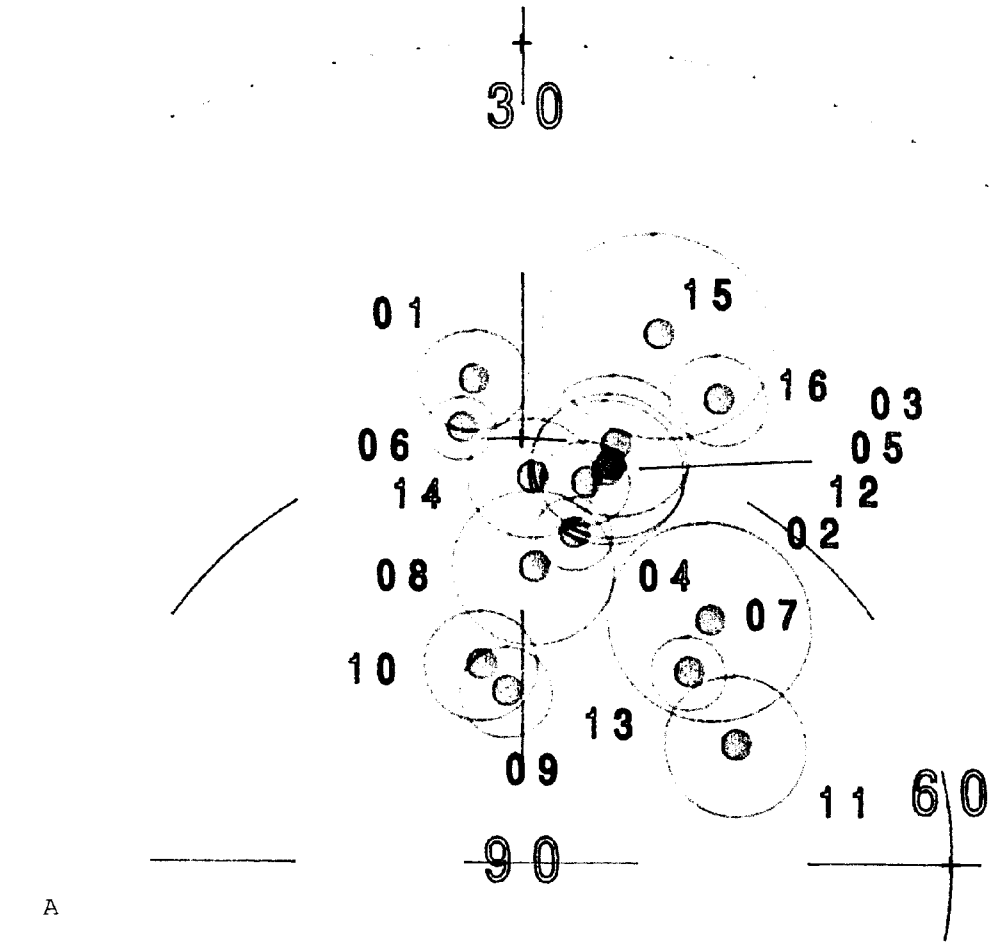

A

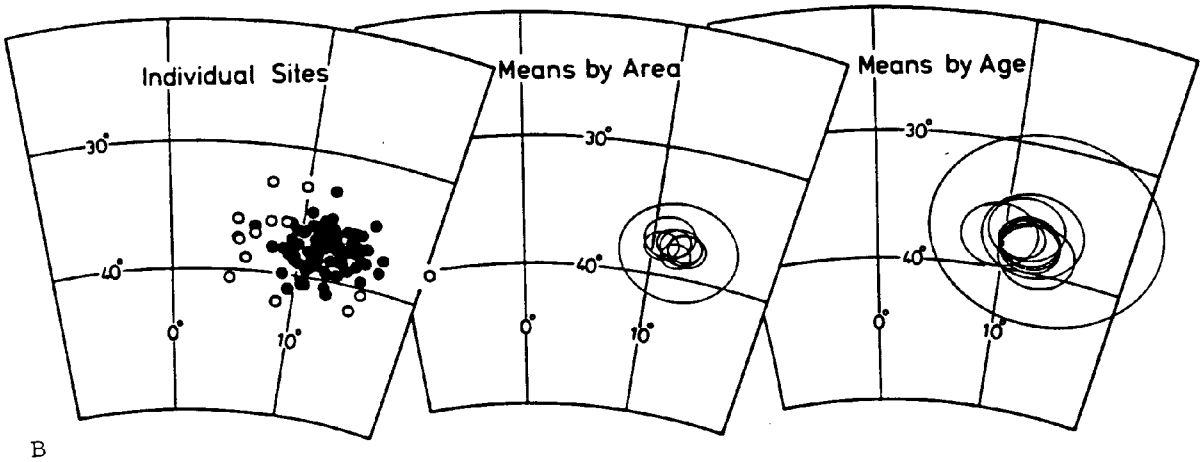

B

Fig. 14 Comparison of site dispersion between Hawaiian flows and those from Kamchatka. A) NRM site-mean directions and alpha-95's for flows from Gorely that show greater dispersion than site-mean directions for sites at Kilauea (B) (Holcomb et al., 1986).

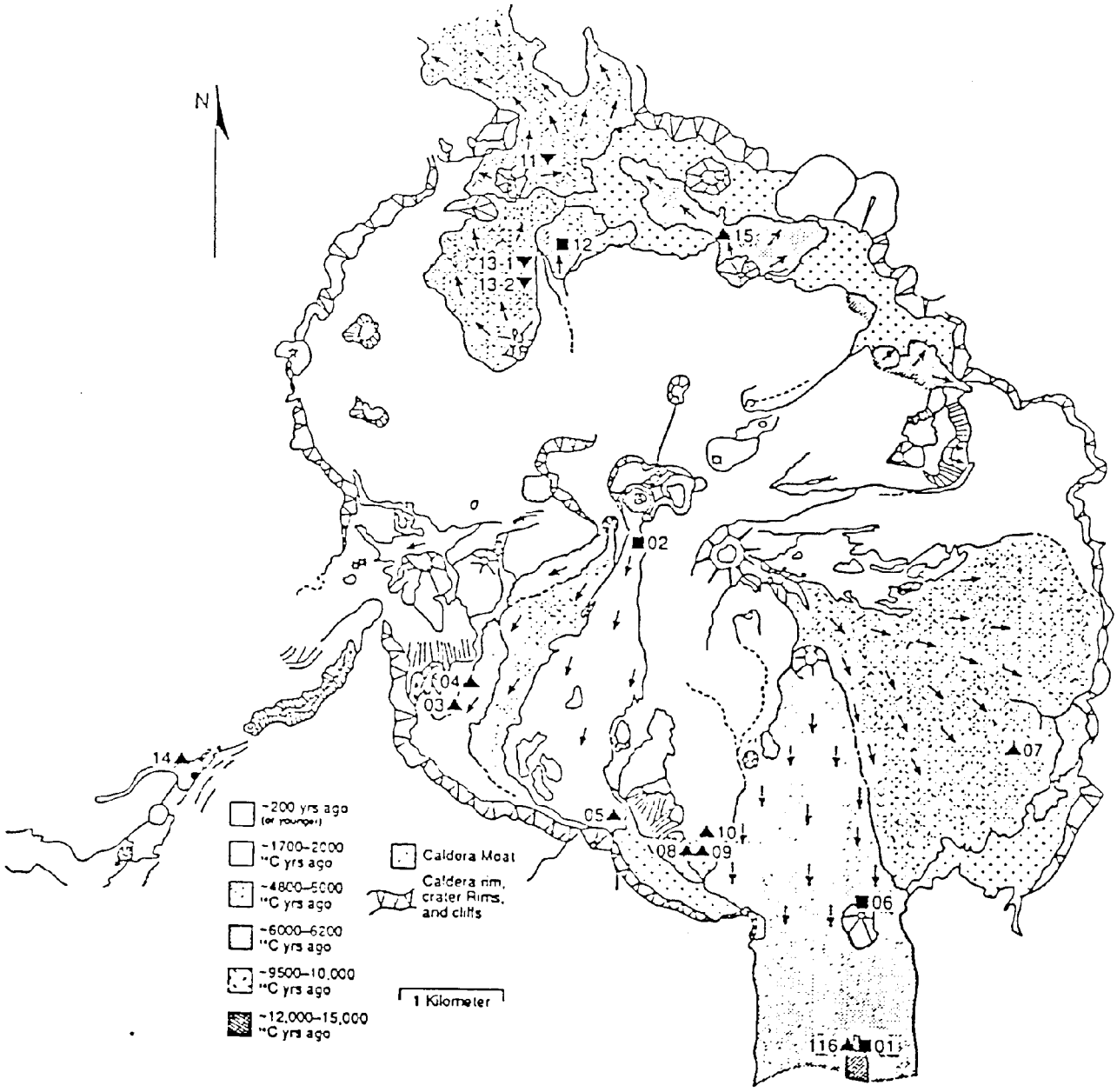

Fig. 15 Map showing location of sites at Gorely Volcano. Symbols indicating age grouping are the same as those used in Figs. 11 and 12 (Burmester, unpublished).

A

Fig. 16 Samples were collected in areas that were least likely to have been transported or tilted after cooling such as A) pull aparts, as seen at site 10 or, B) levees, as seen at Site 12.

B

Core azimuths were calculated from the sun compass and magnetic azimuth readings. Eleven to twenty cores were taken from each site.

Preparation, demagnetization, and measurement

Cores from each site were cut into 1 to 3 specimens, 2.2 cm in length, with a rock saw that was fitted with a diamond-studded copper blade.

Two specimens from each site were used as pilots. One pilot from each site was subjected to step-wise thermal demagnetization and the other to step-wise a.f. demagnetization. Thermal demagnetization was in a custom built oven and a.f. demagnetization was in an Schonstedt AC tumbling-specimen demagnetizer. Magnetization was measured on a Schonstedt spinner magnetometer, model SSM-1A, that was interfaced with a microcomputer.

Samples were demagnetized until they lost an order of magnitude in intensity or until their directions changed erratically from step to step. Intensities for eight to ten levels of demagnetization were recorded for each specimen.

Following analysis of the pilot results, which showed peculiar dispersion, 5 to 6 specimens per site were thermally demagnetized. Further demagnetization was not continued for sites 1, 6, 15, and 16. Demagnetization was not continued for 1 and 6 because these sites showed lower dispersion than other sites and so would not have

benefited us in our search for causes of scatter. Site 15 and 16 were not demagnetized because of time constraints. A.f. demagnetization was not continued because the effects of cooling on magnetization history is the object of study and is best accomplished by studying the behavior of the specimens as they are thermally demagnetized.

Temperatures to be used for demagnetization were predicted by plotting temperatures used for the pilots versus the ratio of intensity at the temperature of demagnetization to the NRM measurement of the sample (J/Jo) (Fig. 17). These plots made it easier to estimate demagnetization temperatures for sites that had samples with a wide range of blocking temperatures.

Early results demonstrated that some specimens were getting remagnetized in the oven. The wide range of blocking temperatures in specimens apparently caused some specimens, that were demagnetized at low temperatures, to be remagnetized. This remagnetization was due to magnetic fields in other specimens that were not yet demagnetized. To identify when a specimen was getting remagnetized in this way, specimens were repositioned so that the magnetic field produced by neighbors would be different at each step. The chance for remagnetization was reduced by increasing the separation of the specimens (Fig. 18). In this way, the magnetic field produced by specimens with high intensities had less chance of affecting adjacent specimens.

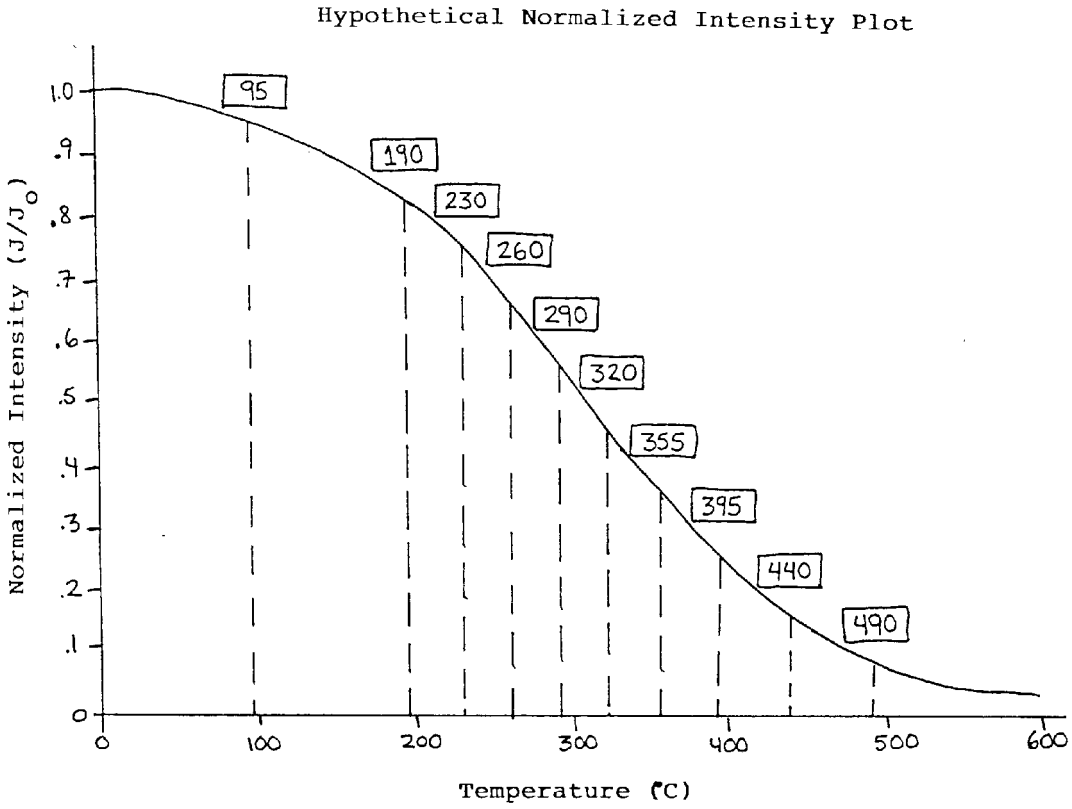

Fig. 17 Hypothetical normalized intensity plot. Specimens from each site are step-wise demagnetized at temperatures determined from plotting pilot demagnetization temperatures against normalized intensity. The steepest part of the curve on the graph is of most interest because the greatest loss of intensity is in this area. The range of temperatures over which the greatest loss of intensity occurs denotes the range of blocking temperatures for the specimen and so a greater number of measurements in this temperature range would give a better determination of the demagnetization path. The temperatures in boxes are those used for other specimens in the site based on the pilot results.

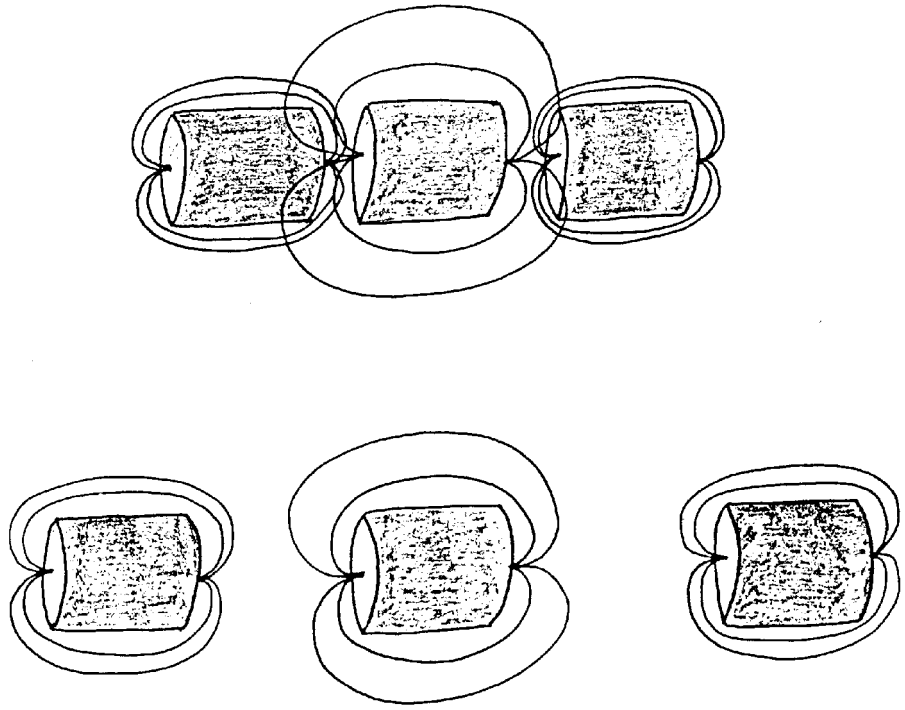

Fig. 18 Some specimens showed remagnetization in the oven. A) Shows a specimen of higher intensity between specimens of lower intensity. The specimen of higher intensity remagnetizes those of lower intensity. B) Distance between specimens is increased to decrease the effect of the higher intensity specimen on the lower intensity specimens.

After magnetizations were measured in the spinner magnetometer, susceptibilities were measured with a Bartington magnetic susceptibility meter. The susceptibilities were monitored to indicate whether oxidation or heating was forming new magnetic minerals. Samples were placed within a magnetic shield when awaiting demagnetization or measurement to inhibit remagnetization by the Earth's magnetic field.

Analysis of Data

Magnetic measurement data were analyzed with the aid of orthogonal plots for each specimen. These orthogonal plots were used to determine the possible number of magnetic components. Best fit lines were calculated by a least-squares method for these components (Kirschvink, 1980). Components plotted on equal-area diagrams graphically revealed within-site dispersion.

Results

Specimens from all sites have high intensities of magnetization. Magnetic directions for all specimens remained stable during step-wise demagnetization, and signal to noise ratios were high. Gamma-95's (Briden and Arthur, 1982) for most specimens were less than 15 degrees, indicating that the magnetizations were homogeneous.

Susceptibilities of all thermally demagnetized specimens, except original pilots, were measured initially and after each demagnetization step to indicate if specimens were being altered during demagnetization. The susceptibilities remained fairly constant through demagnetization. Susceptibilities for most specimens showed fairly constant values which indicates that thermally-induced change was small. Most specimens showed an initial increase in susceptibility which is probably due to annealing, which allows domain walls of large grains to move more easily by relaxing energy barriers. The subsequent decrease in susceptibilities is probably due to oxidation of magnetite to hematite (Fig. 19).

Normalized intensity plots show that most sites contain specimens with broad unblocking temperature ranges . The steepness of the curve is inversely proportional to the range of temperatures over which the specimen was demagnetized (Fig. 20). Normalized intensity plots give us a demagnetization history for the specimens that reflects the approximate range of temperatures over which the specimens were magnetized.

Normalized intensity plots were made for 5 to 6 specimens in each site. All specimens from a site were plotted on a single graph. These plots fall into four general patterns (Fig. 21). Sites 2, 3, and 5 are illustrated by Fig. 2la. Specimens within these sites have low blocking temperature spectra. These blocking temperature spectra show that an order of magnitude of

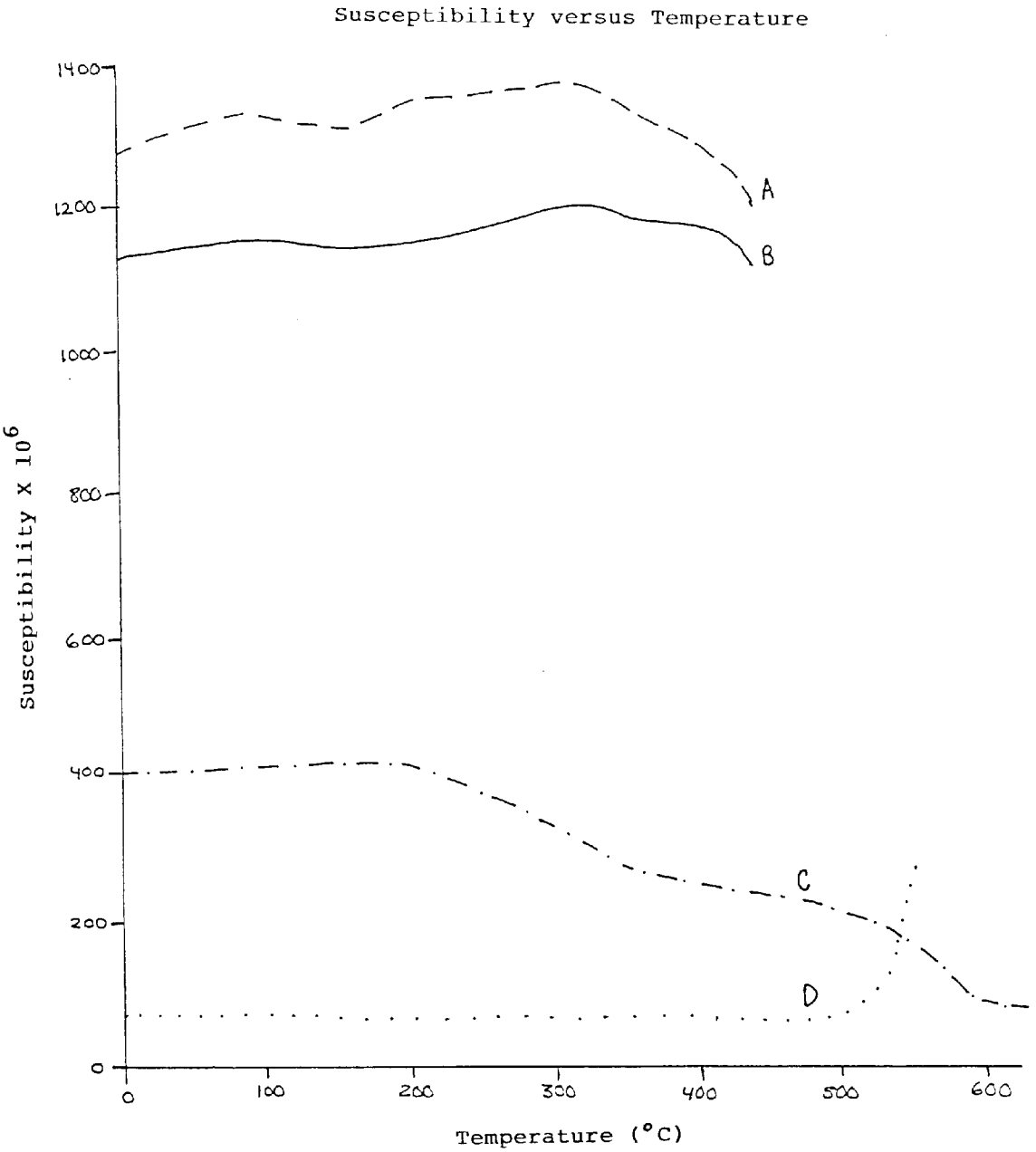

Fig. 19 Plot of susceptibility versus temperature. A) and B) are specimens from Gorely Volcano and C) and D) are from older volcanic rocks. The absolute changes in C and D are proportional to that of A but their changes are phenomenal compared to their own changes in susceptibility. The decrease in susceptibility for specimen C) can be explained if heating oxidized magnetite to low susceptibility hematite. The sharp increase in susceptibility for specimen D is due to low susceptibility iron sulfides being oxidized to magnetite.

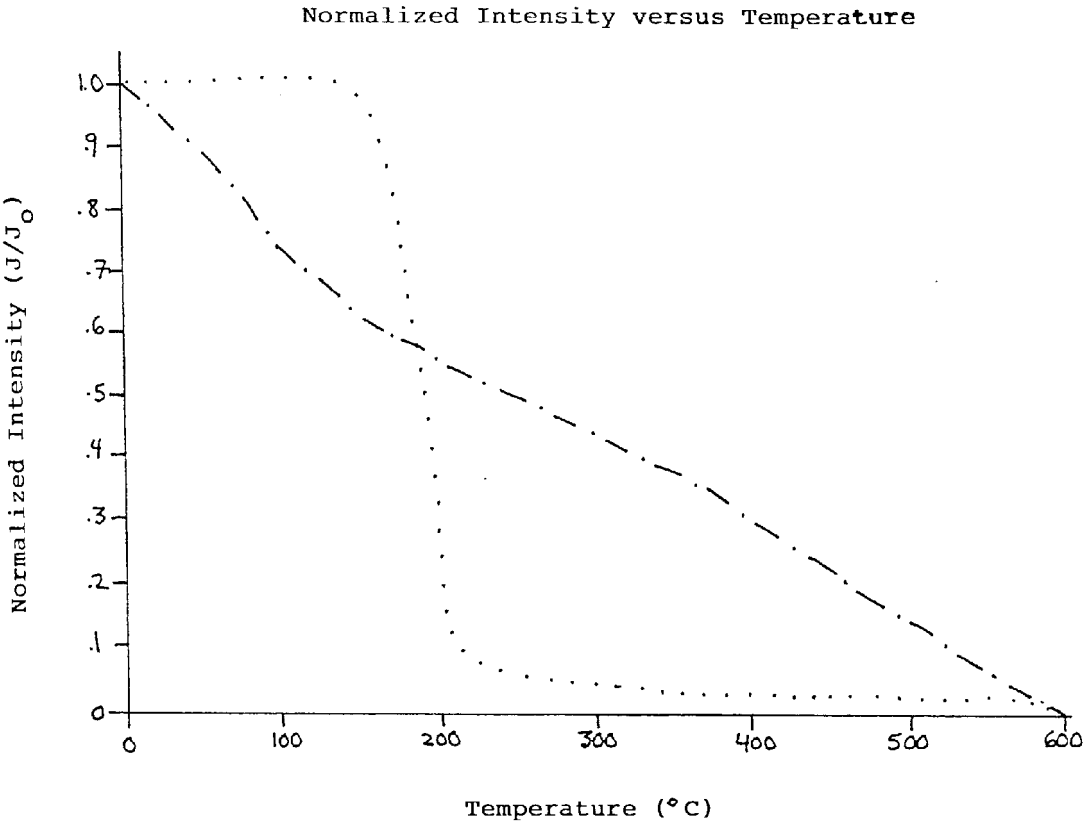

Fig. 20 Plot of normalized intensity versus temperature shows how steepness of curve varies inversely with the blocking temperature range. A small blocking temperature range would produce a steep gradient (dotted line) and a large blocking temperature range would produce a shallow gradient (dot-dash line).

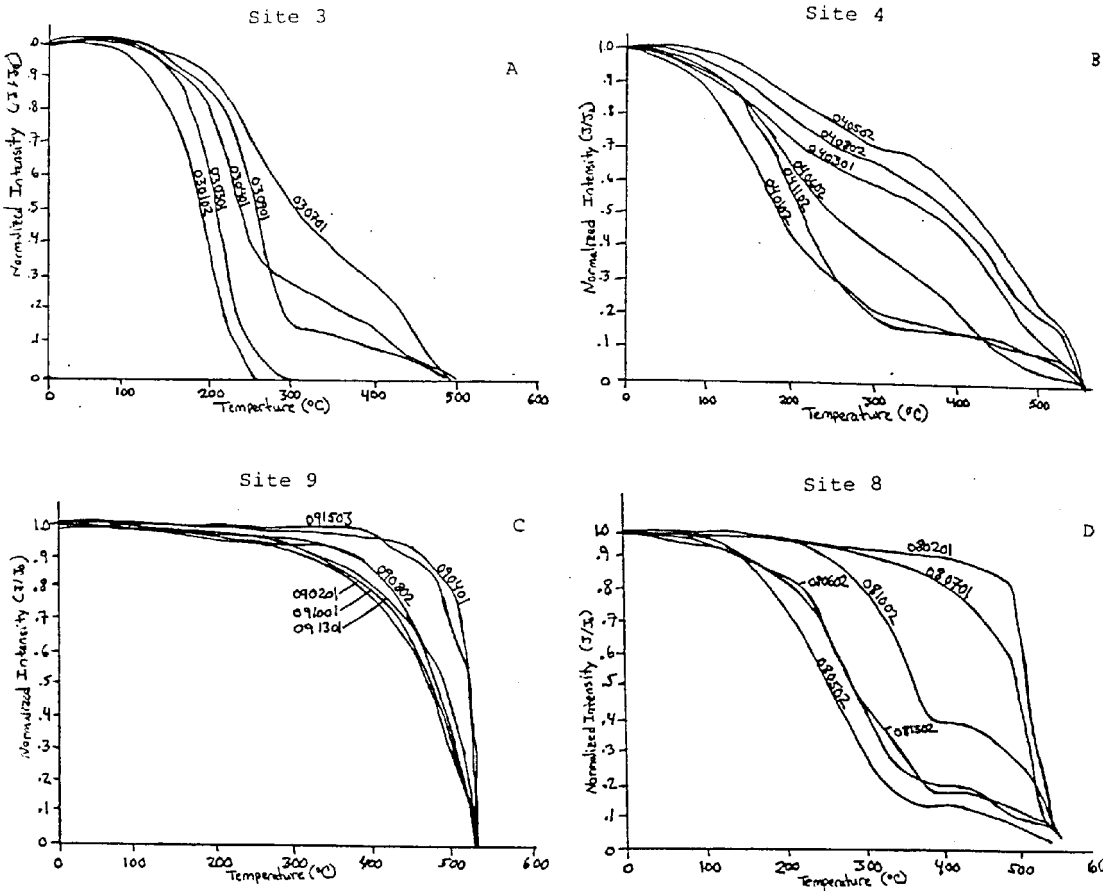

Fig. 21 Plots of normalized intensity versus temperature showing the four patterns seen in sites at Gorely Volcano. A) shows low blocking temperatures, B) shows broad blocking temperatures, C) shows high blocking temperatures, and D) shows a wide range in blocking temperature spectra.

intensity is lost over a range of 100 to 160°C. This loss of intensity occurs at temperatures of 160-360°C or 250-440°C. A second pattern(Fig. 21b) is exhibited by sites 4, 7, and 13. The blocking temperature spectra of these sites are broad, with an order of magnitude in intensity lost over a range of 300 to 400°C. The broadest range of blocking temperatures is from site 4. Site 4 is also the site that shows the least amount of scatter of directions. A third pattern (Fig. 21c) is shared by sites 9, 10, 11, and 12. The blocking temperature spectra in these sites are not as broad as those for sites 4, 7, and 13. An order of magnitude in intensity is lost over a range of 60 to 120°C; demagnetization occurred between 320 and 560°C. A fourth pattern (Fig. 21d) is exhibited by sites 8 and 14. Specimens within these sites did not demagnetize in similar fashions. In site 8, for example, specimen 080201 lost the majority of its magnetization between 480 and 540°C, but specimen 080502 was effectively demagnetized between 120 and 370°C. Sites 8 and 14 showed more scatter of directions than other sites.

Most orthogonal plots show magnetic measurements plot on a straight line through the origin, indicating that most specimens have a single magnetic component (Fig. 22). Two exceptions are worth noting: irregular paths at low temperature and irregular paths at high temperature. Plots for specimens that exhibit irregular paths at low temperatures indicate an irregular change

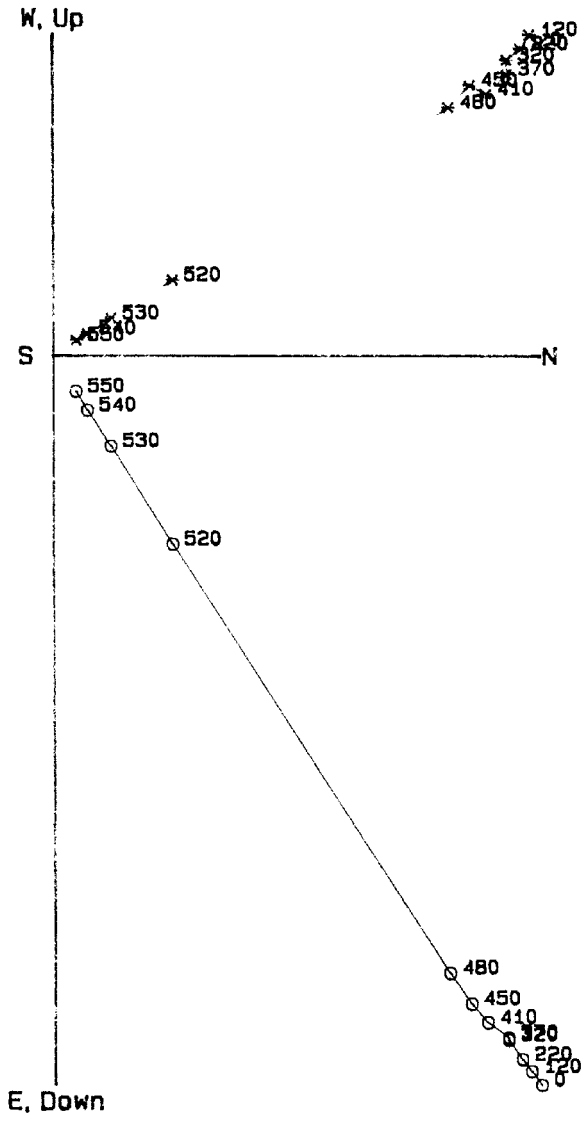

Fig. 22 Orthogonal plot showing single magnetic component. Most specimens show a straight demagnetization path that trends toward the origin.

in magnetization with little progressive demagnetization (Fig. 23). The origin of this behavior is not understood, so low temperature data were considered unreliable and only higher temperature measurements were used to define the magnetic components.

The other exception is that a few specimens show irregular paths at high temperatures (Fig. 24). As mentioned before, remagnetization of some specimens in the oven may be attributed to contrasts in unblocking temperature spectra and large differences in intensities. Rapid direction changes or zigzagged line patterns on the orthogonal plots in the high temperature ranges for some specimens probably reflects this remagnetization.

With the exception of some of the low and high temperature measurements, the remaining measurements were highly linear. This is reflected by small maximum angular deviations or MAD's (Kirschvink, 1980). Lines fit to these measurements trend toward the origin. These observations are consistent with the representation of magnetization as single-component. Single-component magnetization is also reflected in equal-area plots where directions for specimens after demagnetization are similar to the NRM directions for those specimens, i.e.directions did not change. In this paper, figures of equal-area plots use NRM directions based on the assumption that all specimens maintain their current direction (or at least very close to their current direction) after demagnetization.

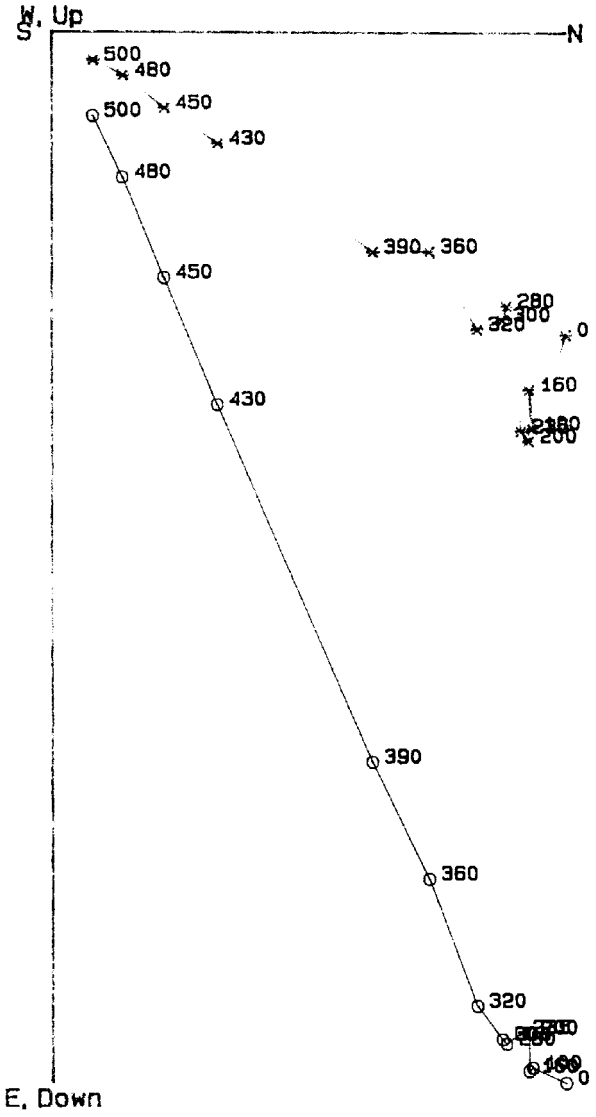

Fig. 23 Orthogonal plot shows zigzagged path at low temperature. Low temperature data showing this irregular magnetization path were considered unreliable and were not used to define the magnetic components for specimens.

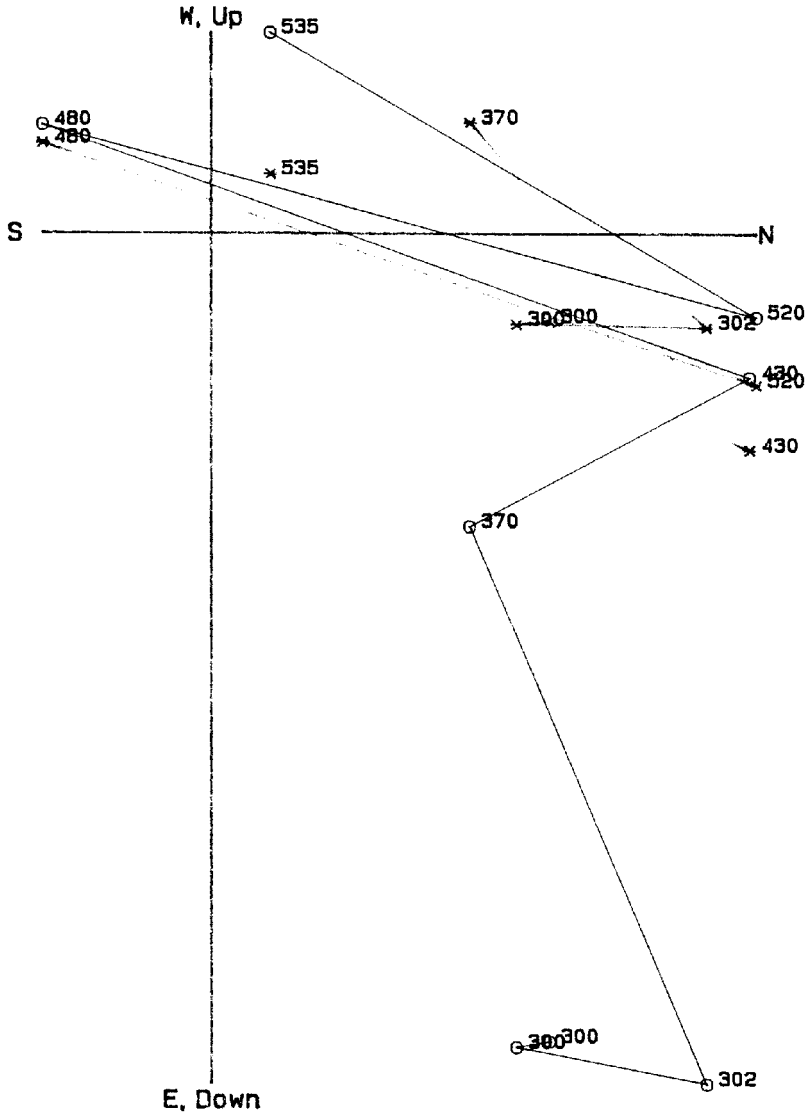

Fig. 24 Orthogonal plot shows remagnetization at high temperatures of a specimen due to contrasts in unblocking temperatures and large differences in intensities of other specimens. Notice that this is a "blow up" of the high temperature data and does not show the whole demagnetization path.

Some specimen directions within a site plotted on equal-area nets show elongate distributions or linear patterns (Fig. 25). These distributions in specimen directions produce the within-site scatter that is the focus of this study. Elongate distributions could be due to two magnetic components contributing in various degrees to the magnetic direction of the specimen. This is not the case for the sites in this study because only single-component magnetizations were observed. These distributions might be explained by differential movement after acquisition of magnetization or systematic changes in the magnetic field generated from a magma-induced electrical current.

Discussion

To simplify investigation of the scatter, it is assumed that scatter is due either to the magnetic field changing direction with respect to the sample, or the sample changing orientation with respect to the earth's magnetic field (Fig. 26). The first assumption might apply to situations where part of the magnetic field is due to an electrical current being generated by lava flowing within a near-by channel. The suggestion that an electrical conductor within the earth's magnetic field generates another magnetic field that affects specimen directions and causes them to be scattered, has been proposed by some. This suggestion is highly speculative

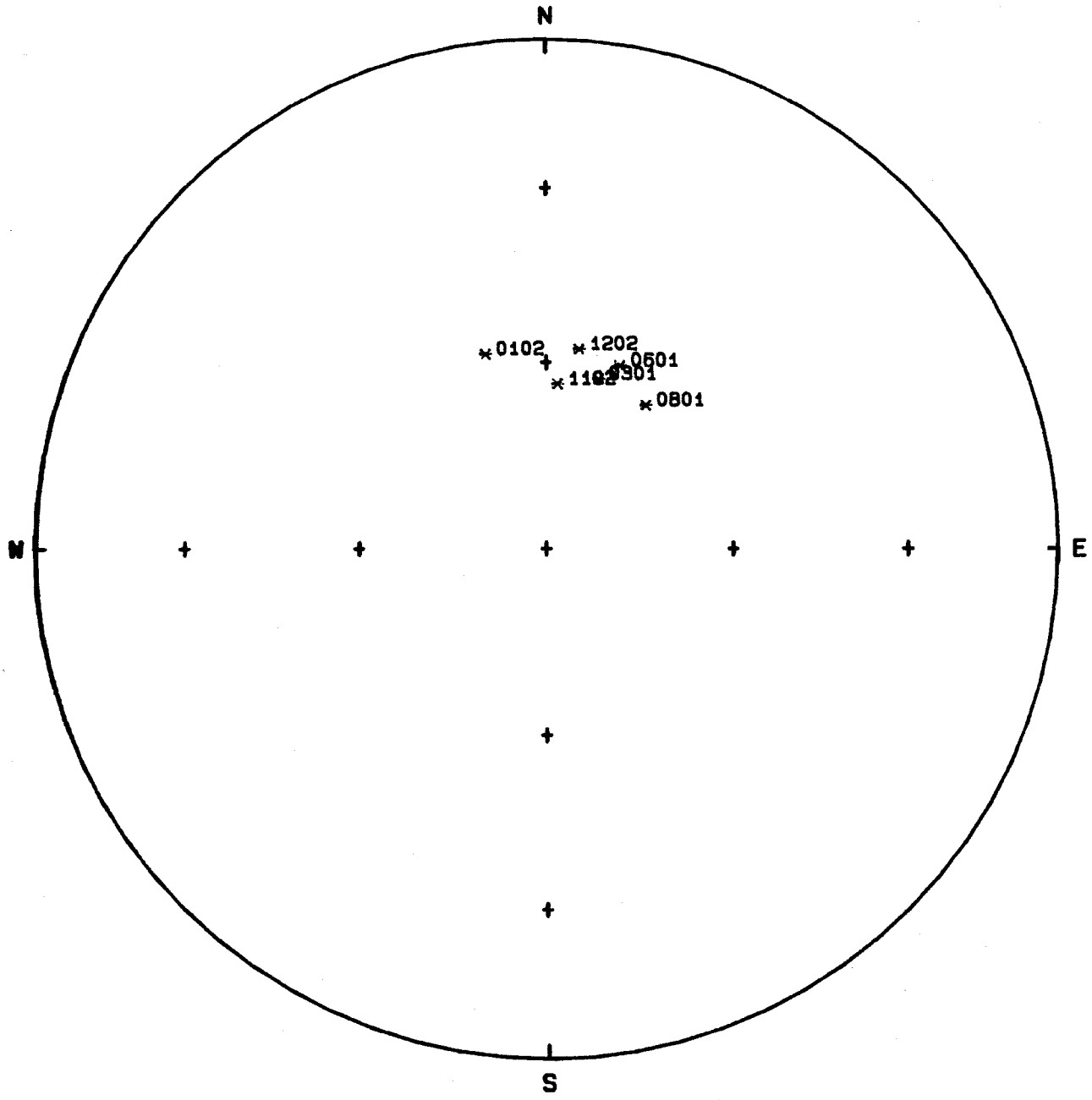

Fig. 25 Equal-area plot of demagnetized specimens at Site 5. Elongate distribution of specimen directions may indicate differential movement after specimens obtained their magnetic directions.

Streak exaggerated (worse) if magnetic orientations used instead of sun compass.

Streak exaggerated (worse) if magnetic orientation used instead of sun compass

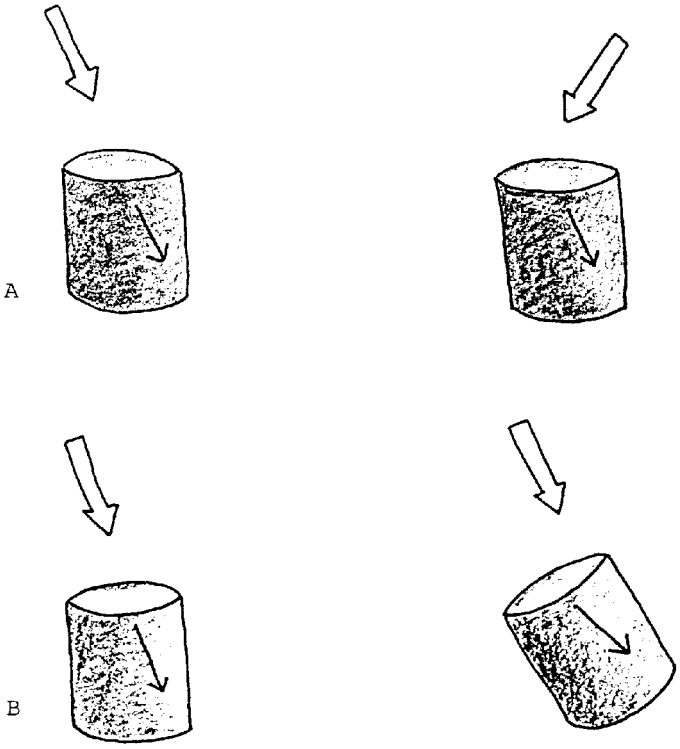

Fig. 26 A) Cartoon of the magnetic field (large open arrow) changing direction with respect to the sample and B) the sample changing orientation with respect to the magnetic field. The arrow within the rock on this and following illustrations represents magnetization acquired earlier.

and needs to be studied further. In this paper, the use of magma-induced electrical currents to explain scatter is only suggested if all other explanations for scatter prove negative.

The second assumption for scatter is that the sample changed its orientation with respect to the earth's magnetic field. This could result from rafting of surface lava that cools faster than lava within the middle of the flow, or from tilting or rotation of surface blocks (Fig. 27 and Fig. 28). The material sampled might also have moved due to lava tube expansion or lava oozing out through surface lava, chilling, and rolling over.

Originally it was assumed that low temperature measurements were more likely to show the correct magnetic field direction. It was assumed that the directions obtained at low temperatures would reflect the magnetic field direction better than directions obtained at higher temperatures because specimens at high temperatures had a greater chance of being moved or being affected by magma induced electrical currents than those at low temperatures (Fig. 29). Because demagnetization over low temperature ranges did not yield reliable components of magnetization, we can not rely on them to give us the best record of the magnetic field direction. When these measurements are excluded, most specimens show only single-component magnetization.

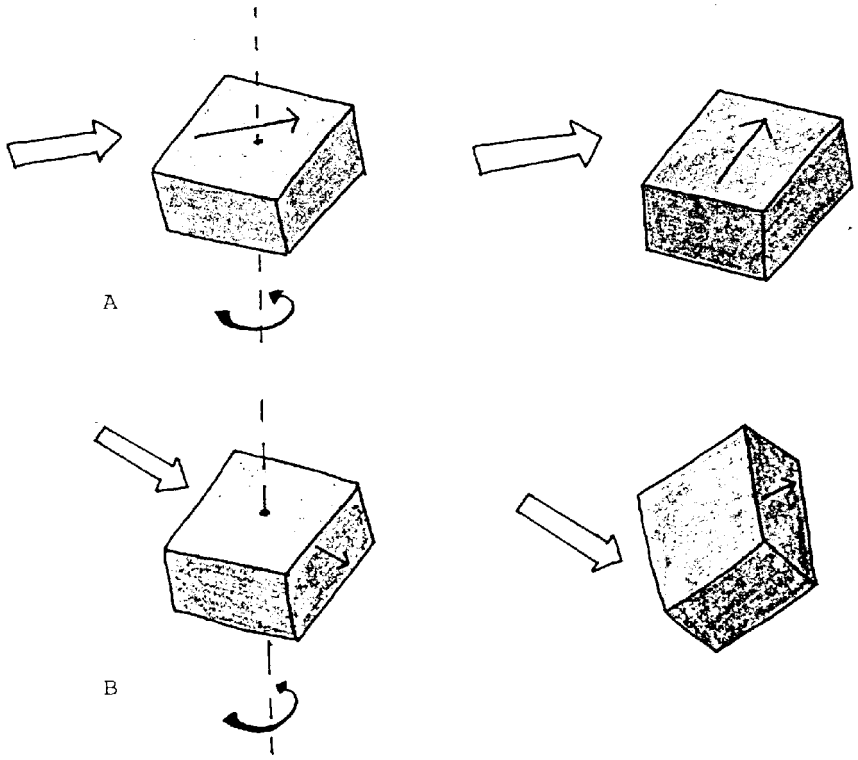

Fig. 27 Movement of the sample after obtaining its magnetic direction by A) rotation about a vertical axis and B) a combination of tilting and rotation.

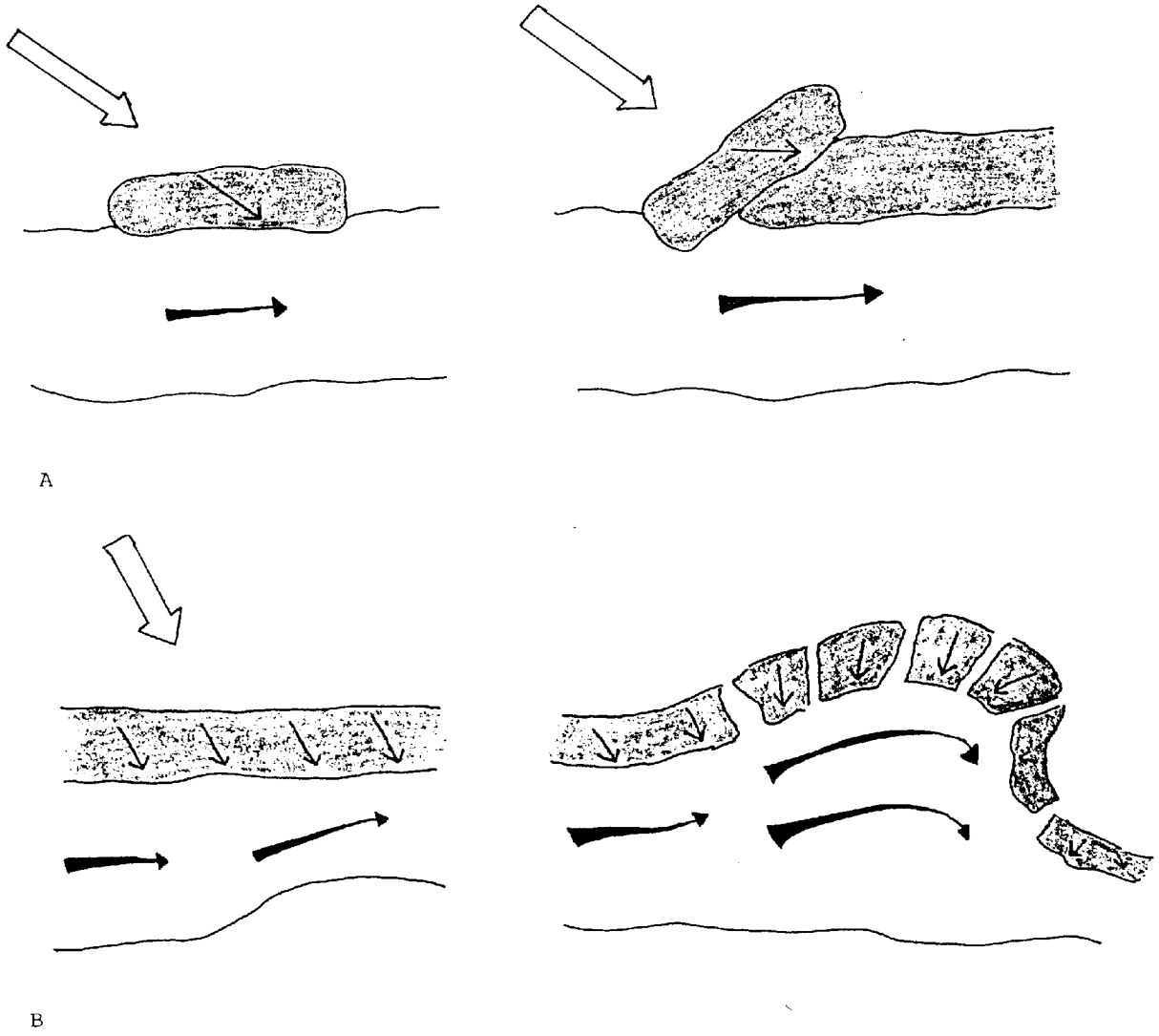

Fig. 28 Cartoon showing movement of the sample by A) rafting of surface lava and B) surface lava rolling over as lava oozes up.

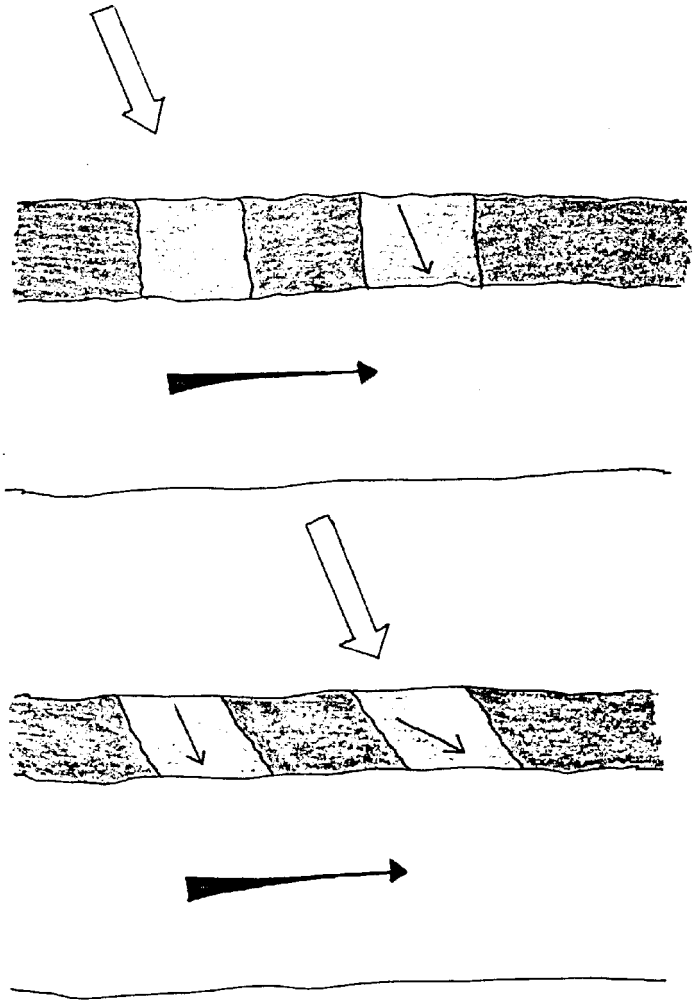

Fig. 29 Cartoon illustrates how a sample with high blocking temperatures might be rotated so that its magnetic direction does not match that of the magnetic field but a sample with low blocking temperatures obtains its magnetic field direction after rotation and so matches the magnetic field direction.

Single-component magnetization indicates that the magnetic field direction did not change with respect to the specimen during magnetization. If the scatter is due to the specimen moving in the earth's magnetic field, then the specimen must have moved after acquiring its magnetic direction and not while acquiring its magnetic direction. Likewise, if the scatter were due to the magnetic field changing with respect to the specimen, it would have changed after but not during the time the specimen was acquiring its magnetic direction.

The history of movement or change in the magnetic field for specimens at a site is complicated because it is not known when the magnetic directions for each specimen was acquired. The question of when one specimen was cooled or emplaced with respect to another can not be answered because there is no simple way to correlate lava from place to place so that relative ages can be determined. The history of movement of specimens or change in the magnetic field at a site is further complicated by the range in blocking temperatures of specimens, the rate of cooling of specimens through their blocking temperatures, and when movement of specimens or change in the magnetic field occurred, i.e., during or after the specimen acquired its magnetic direction. As mentioned before, the latter complication can be excluded since most specimens show only single-component magnetization.

Blocking temperature ranges produce complications because, at high blocking temperatures, specimens are more likely to be exposed to changing magnetic fields induced by a lava flow or are more likely to move than at lower temperatures. This is because the environment in which the specimen is cooling is more likely to be fluid. This would produce scattered specimen directions. Specimens with low blocking temperatures would be less likely to move or be exposed to a changing magnetic field because the environment is less fluid.

Further complications result when specimens have wide blocking temperature ranges. If specimens had acquired their magnetic directions as they were being moved or when the magnetic field was changing, multi-component magnetization should be observed on orthogonal plots (Fig. 30). These specimens would have NRM directions that would show little scatter because the components would be averaged. These directions would become more scattered upon demagnetization. But multi-component magnetization was not observed.

Scatter in the specimen directions for sites with wide blocking temperature spectra may be due to specimens cooling quickly in an environment whose magnetic field is not constant. The specimen would obtain a magnetic direction of the magnetic field generated by a magma- induced electrical current that is present at the time it was cooling through its blocking temperatures. After cooling, the magnetic field direction produced by electrical

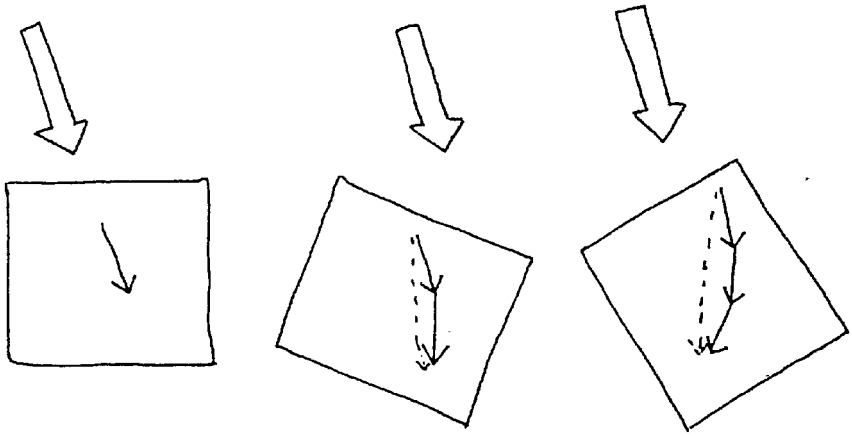

Fig. 30 Illustrates how a sample with a broad blocking temperature range would get its magnetic direction if it were moved while cooling through its blocking temperatures. Open arrows are the direction of the earth's magnetic field. Solid arrow is the magnetic direction obtained in the sample at a certain time period and the dotted arrow is the resultant magnetic direction for the sample.

current would change and the magnetic direction reflected in the specimen would not be the same as that of the current magnetic field direction. Therefore specimens cooling at different times or in different areas would acquire nonuniform magnetic directions because of the changing magnetic field, and scatter would be observed in equal-area plots.

The complications resulting from different blocking temperature ranges are complicated by the other complications mentioned previously and make it difficult to determine how scatter was produced. These combined complications produce various degrees of scatter.

One of the sites with the least amount of scatter is site 6. This site is unusual because samples were taken from the agglutinate of a cinder cone. The low amount of scatter indicates that magnetized samples were not moved, or moved only slightly. The low amount of scatter also indicates that material of the same age was sampled and therefore methods used in sampling are accurate. Changes in the magnetic field due to a magma-induced electrical current would not be expected to have affected specimen directions at this site because there was no lava flowing in nearby channels.

Site 4 had the least amount of scatter and had the widest blocking temperature range of those sites that were demagnetized after initial pilots (Fig. 31). Samples from this site were taken from massive interiors of the lava flow (Fig. 32). With respect to specimen movement,

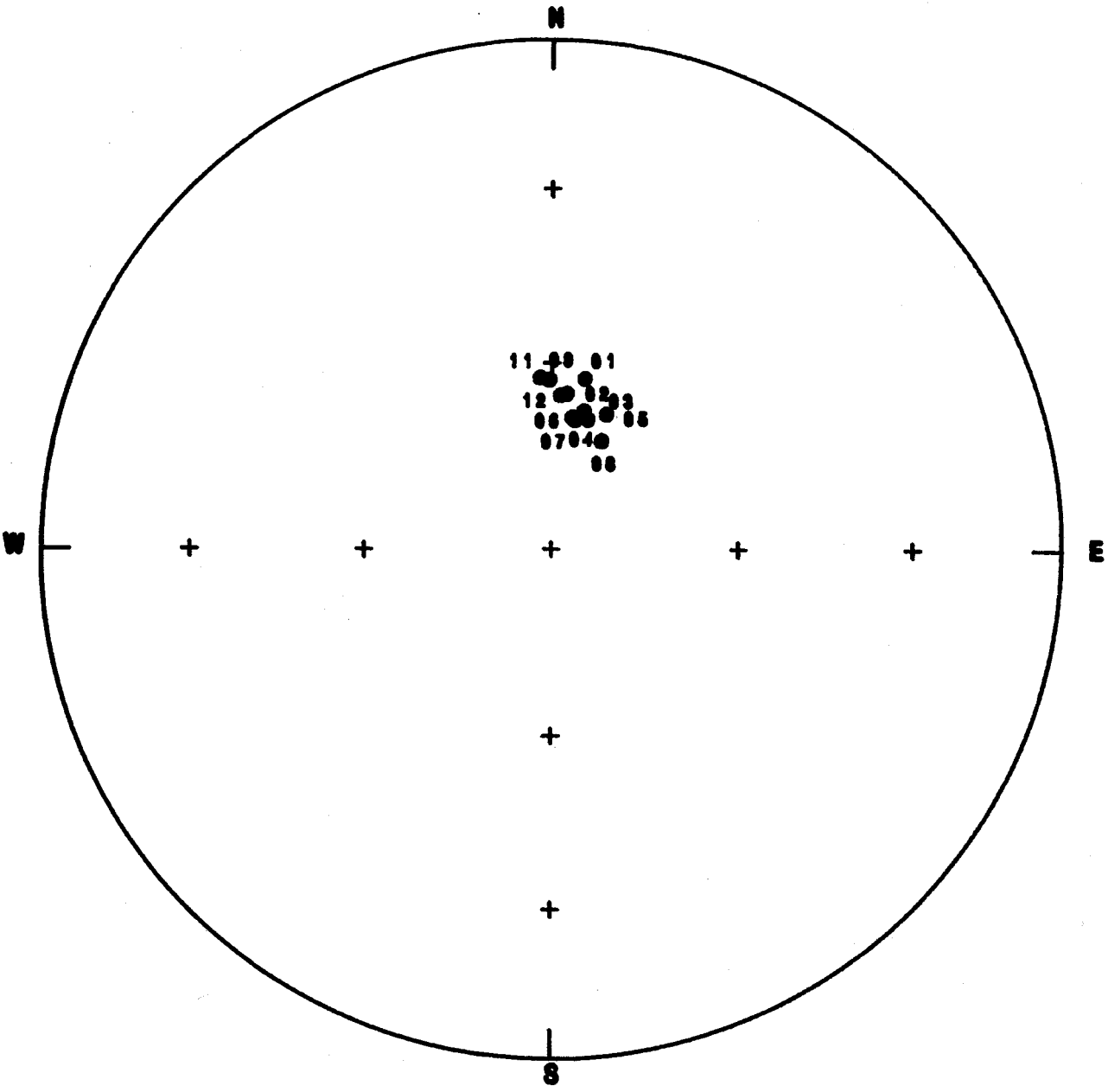

Fig. 31 NRM directions for site 4. Site 4 had the widest blocking temperature range and the least amount of scatter.

Still, after cleaning, 3rd group (9-12) was still most westerly; 2nd group (5-8) most easterly, & 1st in middle, suggesting block rotation or local magnetic anomaly during magnetization.

Still, $\alpha_{95} = 2.6$; fisherian, the look streaked.

Still, after cleaning, 3rd group (9-12) was still most westery; 2nd group (5-8) most eastery, and 1st in middle, suggesting block rotation or local magnetic anomaly during magnetisation.

Still, $\alpha_{95} = 2.6$; fisherian, the look streaked.

Fig. 32 Shows the massive lava flows sampled at Site 4. Low scatter in specimen directions indicates that the massive part of this lava flow did not move.

the low amount of scatter indicates that these massive parts of the flow did not move relative to one another after acquiring their magnetic direction. This indicates that massive parts of a lava flow are less likely to move than surface parts. This perhaps is due to lava no longer flowing or flowing slowly within the channel. With respect to a changing magnetic field, the low amount of scatter would indicate that no changes in the magnetic field occurred at depth. This may be due to there no longer being a strong magma-induced electrical current because lava is no longer flowing or flowing too slowly. This would generate either no magnetic field or a magnetic field that is too weak to affect specimen directions. This site had specimens with wide blocking temperature ranges and single-component magnetizations which indicates that cooling may have taken place over a long period of time and that conditions during cooling must have remained stable. This supports the idea that lava was either flowing slowly or not at all during the time specimens cooled. Site 1 was also sampled from massive interiors of flows and it too showed low dispersion in specimen directions.

Greater dispersion in specimen directions was found at site 3. This site showed obvious patterns of movement by specimens with respect to the magnetic field. Site 3 showed indications that samples might have been tilted when lava oozing out of the toe of a flow caused surface lava to roll over. The rollover can be seen in the

photograph in Figure 33. The equal-area plot of the specimens from this site shows two distinct groups (Fig. 34). One group contains specimens that are identified as surface flow and the other group contains specimens sampled from ooze-out. Surface flow specimens are well clustered, which indicates that they have not moved (at least relative to each other) or have moved only slightly. Specimens from the ooze-out are clustered in two areas on the equal-area plot. If the specimens from the surface flow indicate the true direction of the magnetic field, then specimens from the ooze-out would have been tilted to either the west or northwest. These directions of tilt match well with those observed from the photograph.

Another site might also show movement of the specimen with respect to the magnetic field. Field notes from Site 7 indicate that rifting may have caused lava to tilt to the southwest and northeast. However, when specimens are plotted on an equal-area net (Fig. 35), specimens on opposite sides of the rift are in groups to the northwest and southeast. This is what would be expected if the rift were striking northeast-southwest instead of northwest-southeast. When flows are untilted along the rift striking northeast-southwest, specimen directions move toward each other and scatter is reduced. It is possible that the north arrow was improperly labeled in the field notes causing confusion over which direction the rift is striking.

Fig. 33 View looking west at site 3. The ooze-out can be seen in the center of the photograph, the pahoehoe surface is the light area in the middle right just below the snow.

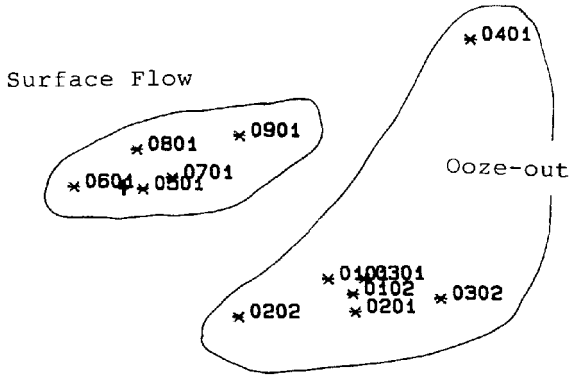

Fig. 34 Enlarged equal-area plot shows NRM directions for Site 3 with middle tick mark at the bottom of the plot equivalent to the center. The tick marks are 30 degrees apart. The specimen directions are separated into two distinct groups. One group contains specimens sampled from surface flow and the other group contains specimens sampled from the ooze-out.

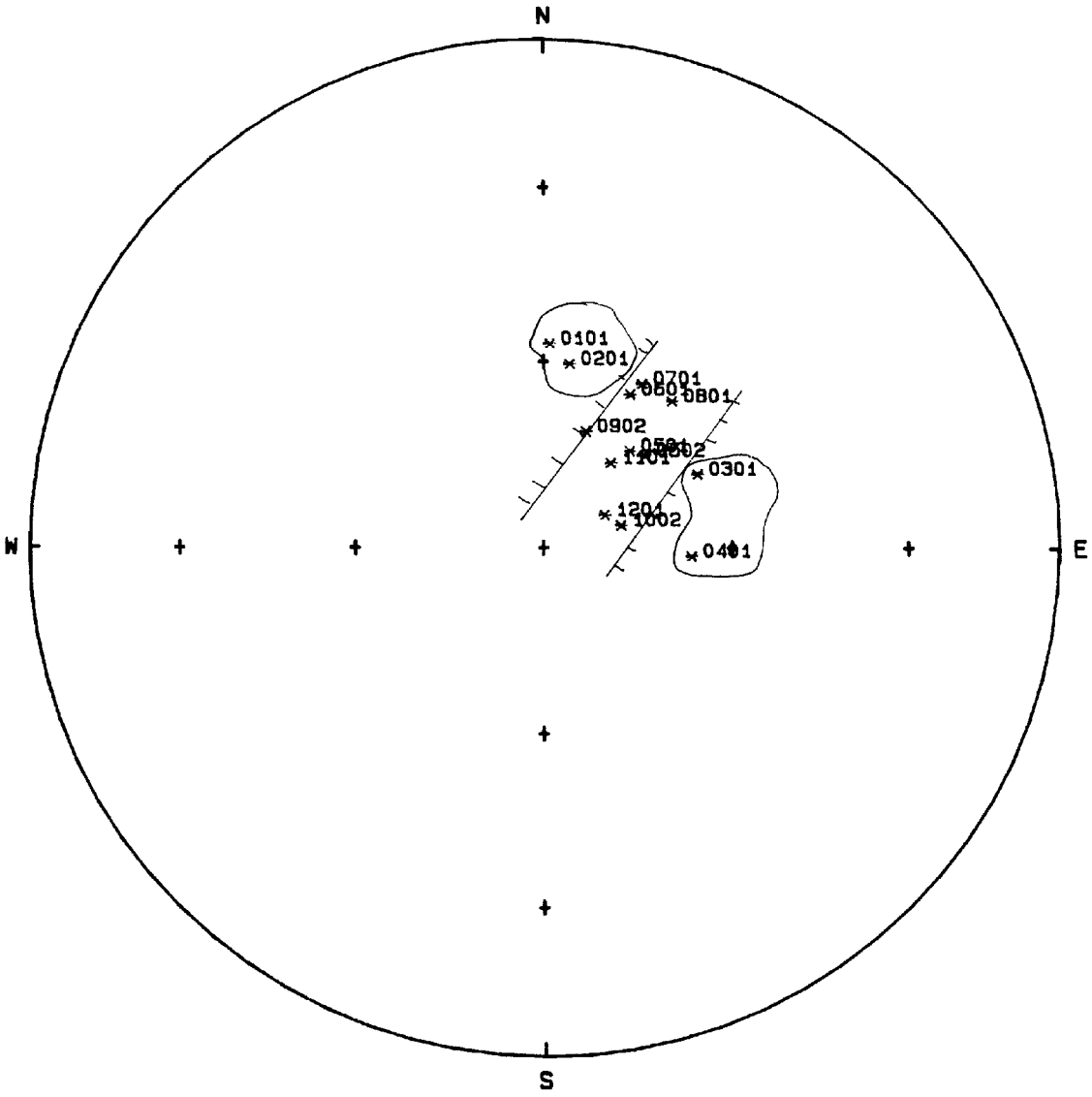

Fig. 35 Equal-area plot showing NRM directions of site 7. Circles show groups of specimens on opposite sides of the rift. The rift is shown striking northeast-southwest.

As mentioned in the results section, several of the sites showed high dispersion in the form ofelongate distributions of specimen directions (see Fig. 24). This type of distribution might indicate differential movement after specimens obtained their magnetic directions or change in the magnetic field during the time spanned by magnetization of the samples.

High dispersion was also found in sites that had levees or pullaparts sampled. These include sites 9, 10, and 12. None of these sites show any mechanism of movement for the sampled material. If the specimen did not move, the only other option for the cause of scatter is that the magnetic field changed.

Over the short time periods in which these lava flows would cool, it has been suggested by some that the only possible change the magnetic field could undergo would be due to the lava flow itself creating a magnetic field. Although the direction of the magnetic field generated by an electrical current within the channel might be predicted, the effects of this field on material external to the channel is not well understood. This means that areas affected by changes in the magnetic field generated by an electrical current can not be identified based on an expected pattern of magnetic directions. Nevertheless, one might guess that if all other explanations for scatter near a lava channel can be ruled out, such a transient field might be the cause.

Site 12 might be an example of scatter due to changes in the magnetic field generated by a magma-induced electrical current. The photograph and reconstruction of this site shows levees that were sampled (see Fig. l5b and Fig. 36). As seen from the photograph, there is no sign that the levees moved, yet the specimen directions are scattered (Fig. 37). If the specimens did not move after acquiring their magnetization the only other option is that the field must have changed and therefore produced the scatter observed in the equal-area plot.

The most scatter in magnetic directions for specimens was found at sites containing specimens with broad ranges in blocking temperature spectra. If all samples cooled simultaneously, specimens with higher blocking temperatures would be more likely to move than those with lower blocking temperatures which would indicate that low blocking temperature specimens would have the least disturbed magnetic direction. If samples did not cool simultaneously, which is the more likely situation, the history of magnetization becomes more complicated and the low temperature specimens are not necessarily the least disturbed. An example of this might be that a low blocking temperature specimen is affected by changes in the magnetic field due to an electrical current or is moved due to the emplacement of a high blocking temperature specimen. The high blocking temperature specimen cools quickly and is not affected by changes in the magnetic field

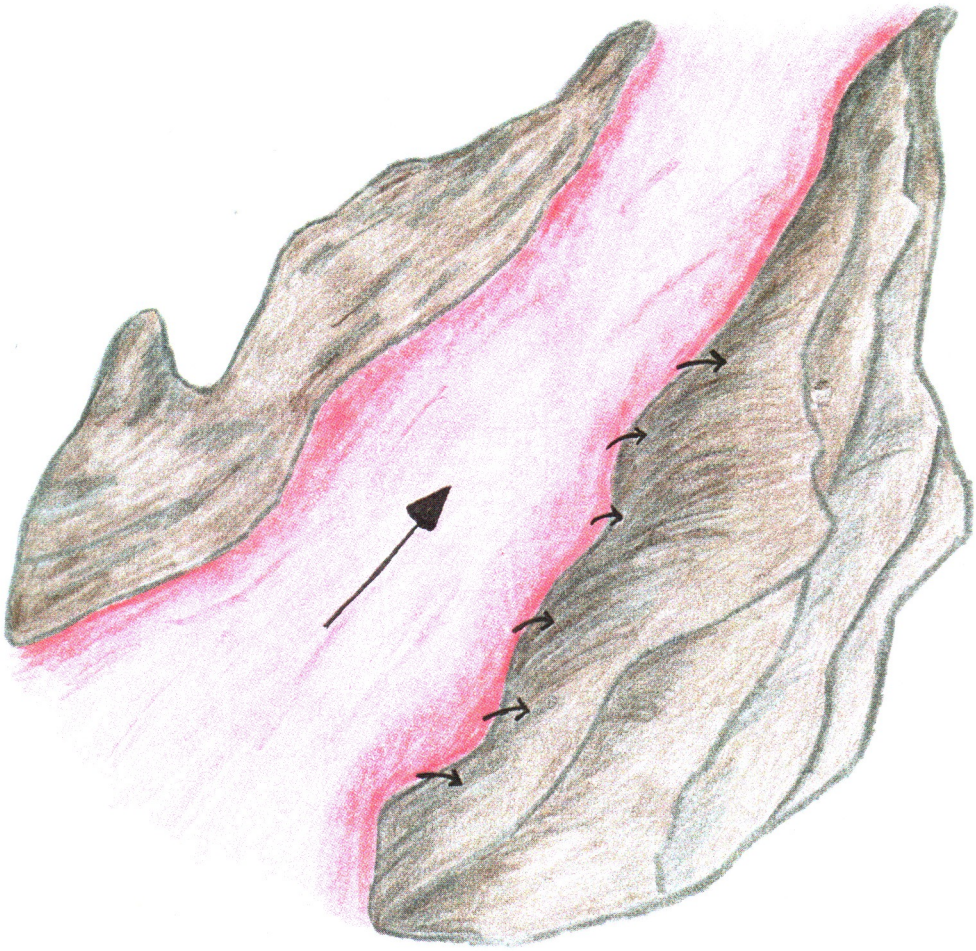

Fig. 36 Reconstruction of Site 12 (see Fig. 15b) showing lava flowing between the levees. As lava travels along the channel in the direction of the large arrow, some of the lava flows over the levees (as indicated by smaller arrows). Samples from these levees indicate that a magma-induced electrical current may have caused changes in the magnetic field and produced scattered directions on equal-area plots.

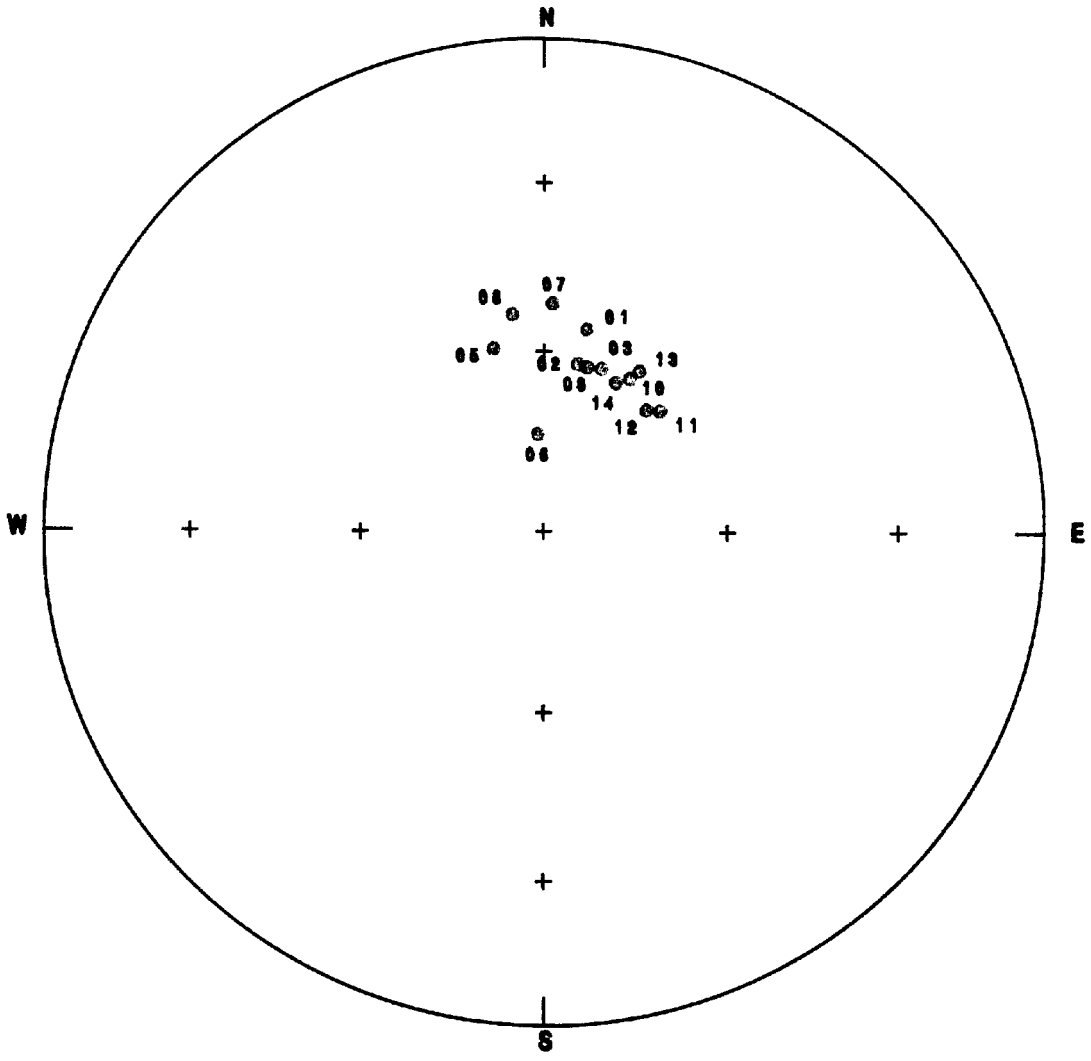

Fig. 37 Equal-area plot of site 12 showing scattered specimen directions.

or movement because lava stops flowing and so the high blocking temperature specimen gives a better magnetic direction for the magnetic field than does the low temperature specimen.

Two sites contained specimens that had a wide range of blocking temperature spectra within the same site. This wide range may be attributed to a range in the amount of titanium in titanomagnetite within the specimens or a range in grain size of magnetite. A specimen with low titanium content in titanomagnetite would have a blocking temperature only slightly lower than pure magnetite, whose Curie temperature is 570 to 580°C. The more titanium in titanomagnetite a specimen contains, the lower the blocking temperature range.

Another possible cause for the wide unblocking temperature range might be that the specimens have a wide range in size of magnetite grains. Very small (single-domain) grains have lower blocking temperatures than do large grains. Single-domain grains maintain their magnetic field direction better than multi-domain grains. This would suggest that samples with low blocking temperatures due to small grain-size would retain a more reliable direction for the earth's magnetic field than samples with high blocking temperatures due to large grain-size.

Specimens of sites showing wide blocking temperature spectra were checked for possible variability in fabric, grain size, or vesicularity. This was because the history

of the magma, and its rate of cooling, might control these factors as well as grain size and titanium content of the magnetic minerals. No fabric, grain size, or vesicularity differences were obvious between specimens within a site. Therefore it is concluded that these factors were not the cause of the wide range in blocking temperature spectra.

Site 8 is one of the sites that contains specimens with wide ranges in blocking temperature spectra (see Fig. 21d). Directions for specimens are highly scattered. Samples 1 through 9 were taken from levees along the lava channel. Samples 10 through 13 were taken from massive parts of the lava flow. As seen on the equal-area plot (Fig. 38), the scatter is very large for specimens 1 to 9 but much smaller for specimens 10 to 13. Since no mechanism for movement can be identified as a source for scatter, changes in the magnetic field are looked to as the source. The wide dispersion of levee directions fits the hypothesis proposed earlier that the surroundings in which the material was deposited was fluid (lava must be flowing in the channel to get material deposited on levees) and therefore samples had a greater chance of being affected by magnetic field changes due to magma-induced electrical currents. The low dispersion in the massive interiors also fits well with the hypothesis that these interiors cooled when there was little or no current produced by the lava flow because by the time the interiors were cooling through their blocking

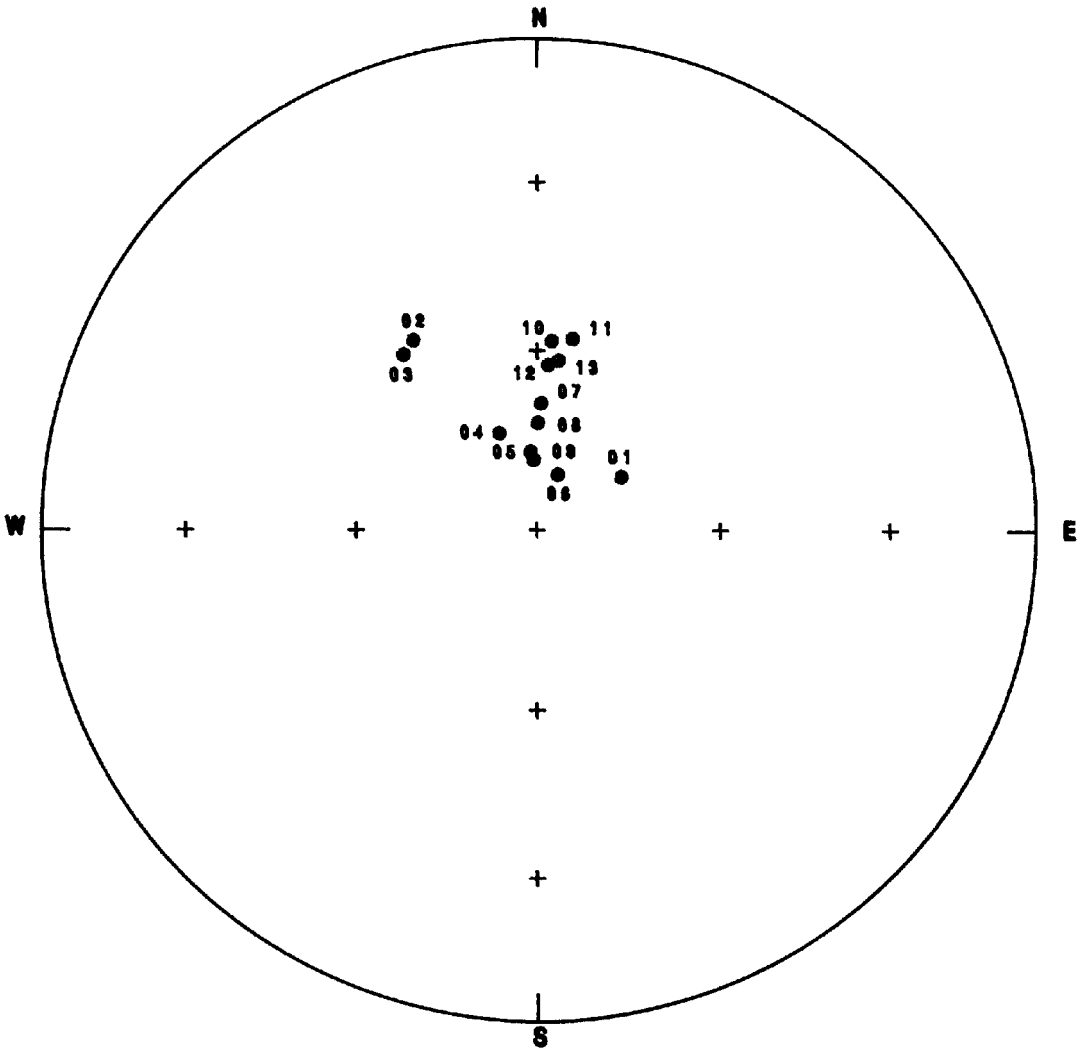

Fig. 38 NRM directions for site 8, which shows wide scatter in specimen directions. Site 8 is one of two sites that had wide ranges in blocking temperature spectra.

temperatures lava was no longer flowing. So changesin the magnetic field did not affect sample directions.

Conclusion

In this investigation, four things were found that might contribute to the high within-site scatter that was observed in samples from Gorely Volcano. These factors are 1) the cooling rate, 2) the range of unblocking temperatures, 3) when a specimen was emplaced with respect to other specimens, and 4)how the specimen moved or was affected by changes in the magnetic field after obtaining its magnetic direction.

It is suspected that changes in the magnetic field had the greater affect on producing scatter than did movement, with the exception of site 3 that showed obvious signs of movement and the possible exception of site 7. Scatter due to changes in the magnetic field are especially evident in sites that had levees or pull-aparts sampled because no mechanism for movement could be identified.

It is suggested that changes in the magnetic field result from magma-induced electrical currents. It is not known how a magma-induced electrical current affects specimen directions. The investigation of this problem is beyond the scope of this paper. Clearly further research is needed in this area.

Nevertheless, even if the above explanation for scatter is found incorrect, the low dispersion in sites 1 and 4 still suggests that massive interiors of lava flows are less affected by movement or changes in the magnetic field than surface parts. This was also noted by Holcomb and others (1986) in their study of Hawaiian lava flows. Other sites were sampled from the surface of flows because there were no outcrops exposing the interiors. These samples showed greater dispersion. This indicates that changes in the magnetic field or movement is more likely to be recorded at the surface than at depth once the material sampled has cooled through its blocking temperature range. This is probably due to lava no longer flowing or flowing slowly when material at depth cools through its blocking temperatures. In future projects, material should be sampled from massive interiors rather than from the surface to avoid the effects due to changes in the magnetic field or movement.

Acknowledgments

I thank Russ Burmester for teaching me the art of paleomagnetism. I especially thank him for the constructive criticism offered while writing this report, the many hours of discussion, and for helping me to understand concepts in paleomagnetism and volcanology. Thanks also to Myrl Beck for encouraging me to do a senior thesis and for classroom instruction that allowed me to better understand the confusing world of magnetics.

References Cited

Berger, G.W., The use of glass for dating volcanic ash by thermoluminescence, Journal of Geophysical Research, 96 (B12), 19,705-19,720, 1991.

Bogoyavlenskaya, G.E., O.A. Braitseva, I.V. Melekestsev, V.Yu. Kiriyanov, and C. Dan Miller, Catastrophic eruptions of the directed-blast type at Mount St. Helens, Bezymianny, and Shiveluch Volcanoes, Journal of Geodynamics, 3, 139-218, 1985.

Braytseva, O.A., I.V. Melekestsev, and V.V. Ponomareva, Age divisions of the Holocene volcanic formations of the Tolbachik Valley, in Fedotov, S.A. and Ye.K. Markhinin, eds., The great Tolbachik fissure eruption: geological and geophysical data 1975-1976, 83-95, 1983.

Briden, J.C., and Arthur, G.R., Precision of measurement of remanent magnetization, Canadian Journal of Earth Science, 18, 527-538, 1981.

Crandell, D.R., D.R. Mullineaux, Potential hazards from future eruptions of Mount St. Helens Volcano, Washington: U.S. Geological Survey Bulletin 1393-C, 26 pp. 1978.

Decker, R.W., The 1980 activity - a case study in forecasting volcanic eruptions, in Lipman, P.W., and Mullineaux, D.R., eds., The 1980 eruptions of Mount St. Helens, Geological Survey Professional Paper 1250, 815-820, 1981.

Holcomb, R.T., Eruptive history and long-term behavior of Kilauea Volcano, in Decker, R.W., and T.L. Wright, eds., Volcanism in Hawaii, v. 1, U.S. Geological Survey Professional Paper 1350, 261-350, 1987.

Holcomb, R.T., D. Champion, and M. McWilliams, Dating recent Hawaiian lava flows using paleomagnetic secular variation, Geological Society of America Bulletin, 97, 829-839, 1986.

Kahle, A.B., A.R. Gillespie, E.A. Abbott, M.J. Abrams, R.E. Walker, G. Hoover, and J.P. Lockwood, Relative dating of Hawaiian lava flows using multispectral thermal infrared images: A new tool for geologic mapping of young volcanic terranes, Journal of Geophysical Research, 93(B12), 15,239-15,251, 1988.

Kirschvink, J.L., The least-squares line and plane and the analysis of paleomagnetic data: examples from Siberia and Morocco, Geophysical Journal of the Royal Astronomical Society, 62, 699-718, 1980.

Leonov, V.L., On some regularities in the development of hydrothermal and volcanic activity in Kamchatka, 28-40, 1990, (in Russian).

Lockwood, J.P. and P.W. Lipman, Recovery of dateable charcoal beneath young lavas: lessons from Hawaii, Bulletin of Volcanology, 43-3, 609-615, 1980.

Mockler, S.B., Russian volcano erupts with little warning, EOS, transactions of the American Geophysical Union, 74(46), 537-539, 1993.

Scott, W.E., Patterns of volcanism in the Cascade Arc during the past 15,000 years, Geoscience Canada, 17, 179-182, 1990.

Wright, T.L. and T.C. Pierson, Living with volcanoes: The U.S. Geological Survey's volcano hazards program, U.S. Geological Survey Circular 1073, 57 pp, 1992.

Zharinov, S.E. and S.S. Demin, Geochemical modeling of the active continental margin: physical nature of volcanism and its relation to seismicity, 3-16, 1989, (in Russian).